

PENNSYLVANIAN CONODONTS AND MICROFACIES FROM NORTHEASTERN MEXICO (TAMATÁN GROUP, CIUDAD VICTORIA BLOCK)

JUAN MOISÉS CASAS-PEÑA¹, PILAR NAVAS-PAREJO^{1*}, UWE JENCHEN²
& JUAN ALONSO RAMÍREZ-FERNÁNDEZ²

¹Universidad Nacional Autónoma de México, Estación Regional del Noroeste, Instituto de Geología, 83000, Bulevar Luis Donaldo Colosio s/n, Hermosillo, México. E-mails: jmoises@geologia.unam.mx; pilarnpg@geologia.unam.mx

²Universidad Autónoma de Nuevo León, Facultad de Ciencias de la Tierra, 67700, Carretera a Cerro Prieto Km 8, Ex. Hacienda de Guadalupe, Linares, México. E-mails: juan.ramirezfn@uanl.edu.mx; uwe.jenchen@uanl.edu.mx

*Corresponding Author

Associate Editor: Francesca Bosellini.

To cite this article: Casas-Peña J.M., Navas-Parejo P., Jenchen U. & Ramírez-Fernández J.A. (2024) - Pennsylvanian conodonts and microfacies from northeastern Mexico (Tamatán Group, Ciudad Victoria Block). *Riv. It. Paleontol. Strat.*, 130(2): 231-258.

Keywords: Biostratigraphy; Morrowan-Atokan; Depositional environments; Del Monte Formation; Peri-Gondwanan Basin.

Abstract. The biostratigraphic analysis of the Paleozoic sedimentary successions in Mexico is crucial for understanding their age, depositional setting, and paleogeographic implications. This study examined conodonts and microfacies of calcareous strata within the Del Monte Formation of the Tamatán Group in northeastern Mexico.

Field observations have led to the identification of three units within the Del Monte Formation: Unit 1, characterized by calcareous sandstone, bioclastic limestone, shale, occasional conglomerate, and dolomitized beds; Unit 2, consisting of conglomerate and/or breccia associated with debris flows; and Unit 3 including turbiditic sandstone and shale.

Conodonts were only recognized in Unit 1, with such genera as *Idiognathoides*, *Neognathodus*, *Idiognathodus* and less frequently, *Streptognathodus*, *Adetognathus*, and *Diplognathodus*. The faunal associations include *Idiognathoides* cf. *Id. corrugatus* Harris & Hollingsworth, 1933, *Idiognathoides sulcatus sulcatus* Higgins & Bouckaert, 1968, *Idiognathoides convexus* (Ellison & Graves, 1941), *Idiognathoides asiaticus* Nigmatganov & Nemyrovskaya, 1992, *Neognathodus* cf. *N. atokaensis* Grayson, 1984, *Neognathodus* aff. *bothrops* Merrill, 1972, *Neognathodus nataliae* Alekseev & Gerelzeveg, 2001 (in Alekseev & Goreva 2001), *Streptognathodus parvus* Dunn, 1966, *Idiognathodus incurvus* Dunn, 1966, and *Idiognathodus* aff. *delicatus* Gunnell, 1931, suggesting Morrowan and Atokan (Pennsylvanian) ages for the dolomitic limestone and grainstone beds.

Five types of microfacies (MF) and several marine facies zone (FZ) have been detected: MF1-bioclastic grainstone and MF2-wackestone deposited at the platform margin (FZ 6 and FZ 7), MF3-dolomitized wackestone representing an inner restricted platform (FZ 8), MF4-mudstone from a deeper water zone (FZ 4), and MF5-siliciclastic beds with bioclasts indicating a high-energy barrier associated with a platform margin (FZ 6). The findings confirm a shallow to deep platform and imply a connection among Mexican peri-Gondwanan basins, including the Tamatán Basin, indicating similarities in sedimentary facies and/or depositional environments linked to the Rheic Ocean during the Early to Middle Pennsylvanian.

Received: January 17, 2024; accepted: May 13, 2024

INTRODUCTION

Paleozoic sedimentary outcrops are limited and sporadic in northwestern, northeastern, central-eastern, and southeastern Mexico. Often these successions overlie Precambrian-Paleozoic metamorphic and igneous complexes and are deformed. Collectively, they constitute the pre-Mesozoic basement of Mexico and define sedimentary basins associated with the different continental terranes or blocks (Ortega-Gutiérrez et al. 2018).

The Ciudad Victoria Block (Ramírez-Fernández et al. 2021), previously considered the northern part of the Oaxaquia superterrane (Ortega-Gutiérrez et al. 2018) and also referred to as Guachichil (Sedlock et al. 1993) or Sierra Madre Terrane (Campa & Coney 1982), includes several outcrops distributed in the northeastern part of Mexico at localities such as Aramberri (Nuevo León), Miquihuana, Bustamante, and northwestern Ciudad Victoria (Tamaulipas) (Fig. 1A).

The most complete exposure of the Ciudad Victoria Block occurs in the Ciudad Victoria area in the Huizachal-Peregrina Anticlinorium, which is part of a large Laramide fold of the Sierra Madre Oriental whose core is being exhumed. The Ciudad Victoria Block consists of four major peri-Gondwanan units: (1) the Neoproterozoic Novillo Complex, which is closely associated with Oaxaquia (Alemán-Gallardo et al. 2019b); (2) the Ordovician Peregrina Tonalite, which is part of the Peregrina-Mochoniano orogen and represents the northern extension of the Famatinian Arc of South America (Alemán-Gallardo et al. 2019a); (3) the Carboniferous Granjeno Complex, representing the accretionary prism of the Rheic Ocean subduction zone, which correlates with the Acatlán Complex and contains a large slab of subducted ocean floor, the Victoria Serpentinite (Torres-Sánchez et al. 2017), and currently remains undated; and (4) the Silurian to Permian Tamatán Group, represented by four predominantly siliciclastic sedimentary formations with a rhyolitic lithodeme. In particular, the Tamatán Group Basin, located in a retro-arc setting between Oaxaquia and Amazonia (Casas-Peña et al. 2021; Ramírez-Fernández et al. 2021), showed a Gondwanan affinity during the Silurian (Boucot et al. 1999; Stewart et al. 1999a). This later shifted to a North American affinity during the Carboniferous-Permian, due to the continuous migration of peri-

Gondwanan blocks and terranes. The migration of these terranes culminated in the formation of the supercontinent Pangea, in the late Paleozoic, as a result of the diachronic closure of the Rheic Ocean and the collision between Gondwana and Laurentia.

The Pennsylvanian sedimentary succession of the Del Monte Formation consists of various marine, both terrigenous and carbonate, facies that played a fundamental role in faunal exchange prior to the consolidation of Pangea. The most important fossils of the Del Monte Formation are microfossils such as *Fusuliniella* sp., *Mirella* sp., *Paramillerella* sp., *Fusulinella* cf. *F. haymondensis* Skinner & Wilde, 1954, corals (*Stereocospha* sp.), and several genera of macrofossils such as goniatites (*Pseudoparalegoceras amotapense* (Thomas, 1928); *Eoasianites* sp.) similar to those from southeastern North America, and with an early to middle Pennsylvanian biostratigraphic age (Murray et al. 1960; Carrillo-Bravo 1961; Gursky 1996). A Desmoinesian age based on conodont occurrences from the Del Monte Formation rocks was reported by Stewart et al. (1999a; N. Savage 1995, written comm.), although they did not include detailed information nor a list of taxa. Therefore, conodonts in the Del Monte Formation have not yet been reported in northeastern Mexico.

This paper aims to report conodonts from the Del Monte Formation of the Tamatán Group from the Ciudad Victoria Block, in Tamaulipas, northeastern Mexico. Biostratigraphy of conodont fauna and their paleogeographic implications are discussed herein, together with a microfacies analysis on the carbonates rocks from the studied sections in a depositional environment frame.

GEOLOGICAL SETTING

The Paleozoic Tamatán Group consists of a more than ~1000 m thick Silurian to Permian siliciclastic and carbonate marine successions (i.e., Cañón de Caballeros, Vicente Guerrero, Del Monte, and Guacamaya formations), and an irregular felsic body (Aserradero Rhyolite). This group is exposed in tectonic contact with the Novillo and Granjeno metamorphic complexes as well as Jurassic successions (Stewart et al. 1999a; Casas-Peña et al. 2021; Ramírez-Fernández et al. 2021; Fig. 1).

The Silurian Cañón de Caballeros Formation is the oldest unit, consisting of conglomerates with

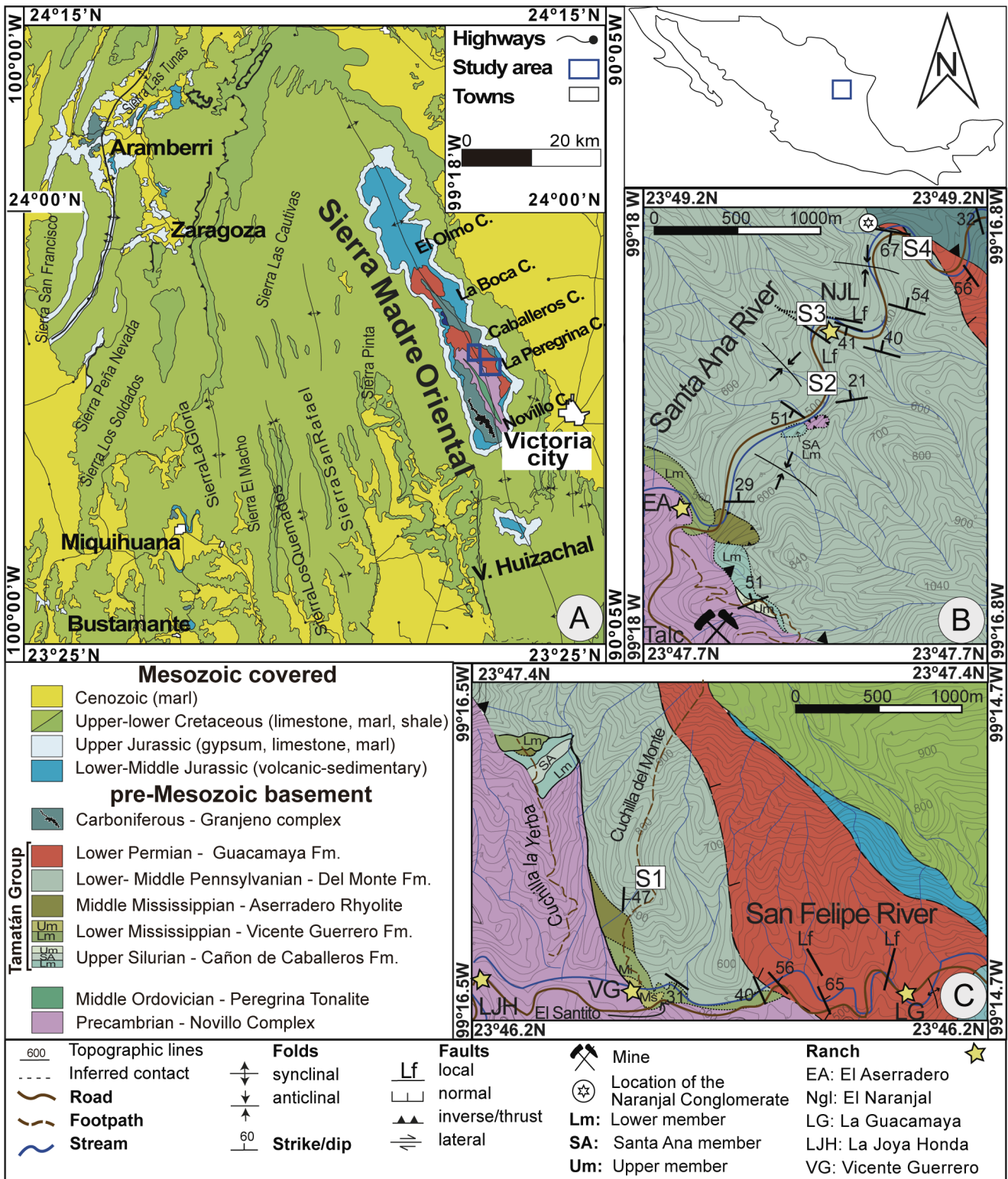


Fig. 1 - A) Pre-Mesozoic basement outcrops of Ciudad Victoria Block in northeastern Mexico and the eroded tectonic window of Huizachal-Peregrina Anticlinorium. Study area in blue-line boxes (modified from Barboza-Gudiño et al. 2011). Geologic maps of Tamatán Group in (B) Caballeros Canyon, and (C) La Peregrina Canyon (modified from Casas-Peña et al. 2021).

volcanic clasts, sandstone as well as limestone with abundant Silurian fauna that includes brachiopods, gastropods, corals, and trilobites. This fauna is similar to the fossil record from the Venezuelan Andes

(Boucot et al. 1997), which indicated that the Tamatán Basin was close to the NW margin of Gondwana in the early Paleozoic (Stewart et al. 1999a; Casas-Peña et al. 2021). Additionally, species of the

genus *Baturria* (Brachiopoda) in the Cañón de Caballeros Formation have also been found in Lower Devonian rocks in Spain, which indicates that this formation can be younger, and is also supported by the presence of younger detrital grain zircon age found in this unit (i.e., 397 Ma; Casas-Peña et al. 2021).

The Lower Mississippian Vicente Guerrero Formation includes conglomerate, sandstone, shale, and silty sandstones with abundant Osagean brachiopods from the shallow marine environments that include *Lamellosathyris lamellosa* (Léveillé, 1835), *Cleiothyridina* cf. *C. tenuilineata* (Rowley, 1900), *Camarophorella* sp., *Punctospirifer* sp., which are similar to the North American Midcontinent fauna (Sour-Tovar & Martínez-Chacón 2004; Sour-Tovar et al. 2005). In contrast to the Silurian faunas, this occurrence indicates a connection between the Tamatán Basin and Laurentia during the Mississippian (Boucot et al. 1999; Stewart et al. 1999a). Based on the provenance data and ~1.5 – 1.6 Ga detrital zircon ages reported by Casas-Peña et al. (2021), a close relationship between the Ciudad Victoria Block, South America (Amazonia), and other peri-Gondwanan blocks (e.g., Maya and Oaxaquia) should also exist.

The Pennsylvanian Del Monte Formation unconformably overlies the Aserradero Rhyolite and the Vicente Guerrero Formation. The Del Monte Formation includes a layer of massive basal conglomerate denominated as Naranjal Conglomerate, medium- to thin- strata of bioclastic limestones with abundant fusulinids (Carrillo-Bravo 1961), and quartz grains (like calcareous sandstone). Likewise conglomerates, sandstones, and siltstones whose geochemical rock compositions comprise a domain of felsic to intermediate sources (Casas-Peña et al. 2021). The Del Monte Formation has been interpreted as the result of a proximal debris flow with the development of turbidite units (Stewart et al. 1999a; Casas-Peña et al. 2021). The Permian Guacamaya Formation has been described as classical synorogenic turbidites (i.e., flysch deposits; Gursky & Michalzik 1989; Gursky 1996). Therefore, this unit is the result of a deep-water deposit, with recorded fusulinids of a Cisuralian age (Carrillo-Bravo 1961), and a concurrent depositional age based on the presence of a younger zircon population (~ 279 Ma; Casas-Peña et al. 2021). The Carboniferous Aserradero

Rhyolite is a lithodeme composed of rhyolitic and rhyodacite bodies with internal flows that were previously described as Devonian novaculites (La Yerba Formation; Carrillo-Bravo 1961). Crystallization age was originally dated in 334 ± 39 Ma (Stewart et al. 1999a), then was further constrained to the Middle to Late Mississippian (347.8 ± 2.7 and 340.7 ± 3.6 Ma). The Aserradero Rhyolite represents the first stage of a pre-collisional Carboniferous-Permian arc (Ramírez-Fernández et al. 2021).

MATERIALS AND METHODS

Fieldwork

The fieldwork was performed along the Santa Ana River in Caballeros Canyon ($23^{\circ}47.7'N$ to $23^{\circ}49.2'N$ and $99^{\circ}16.8'W$ to $99^{\circ}18'W$) and along San Felipe River in the La Peregrina Canyon ($23^{\circ}46.2'N$ to $23^{\circ}47.4'N$ and $99^{\circ}14.7'W$ to $99^{\circ}16.5'W$) where the Del Monte Formation and the Tamatán Group crop out (Fig. 1). Four local stratigraphic sections were examined for conodonts and microfacies based on descriptions by Carrillo-Bravo (1961), Ramírez-Ramírez (1992), and Stewart et al. (1999a). From thirteen samples, six samples from three different sections were productive in conodonts (sections S1, S2, and S3; Fig. 1; Table 1). Conodont analyses were supplemented by 13 thin sections for microfacies analysis (Fig. 3; Table 2).

Section 1 (S1, 60 m-thick) upwards the Cuchilla Del Monte path (Fig. 1C) consists of sub-vertical thick- and thin-bedded bioclastic beds from Unit 1. Occasionally, they are covered by vegetation. At the base of the section, is exposed the contact with the Aserradero Rhyolite (Fig. 2A).

Section 2 (S2, 60 m-thick) is located ~ 1 km to the east of the El Aserradero Ranch along the Santa Ana River in the Caballeros Canyon (Fig. 1B). Medium to thin-bedded grainstone and wackestone beds that occasionally are interlayered with conglomerate, sandstone, dolomitic limestone, mudstone and shale of Unit 1. The most productive conodont sample is in this section (i.e., CC54-08; Fig. 2C).

Section 3 (S3, 15 m-thick) is close to El Naranjal Ranch above the main stream (Fig. 1B). It includes a sandy limestone, bioclastic limestone,

calcarenite, and intercalations of shale and siltstone of Unit 1; occasionally massive package of mudstone as well as intercalations of thin shale and sandstone of Unit 2 (Fig. 2D) and turbidite-like intercalations associated with Unit 3 (Fig. 2F).

Section 4 (S4, 25 m-thick) is located ~1 km east of the El Naranjal Rancho along the Santa Ana River (Fig. 1B). It consists of massive conglomerate, sandstone, and calcarenite beds of Unit 2 (Fig. 2E). At the top of the section the disconformable contact with the Permian Guacamaya Formation is exposed.

Microfacies analysis

Thin sections of thirteen sample rocks distributed among four local sections (S1: 3, S2: 5, S3: 4, and S4: 1) were examined under a polarizing microscope for the microfacies analyses (MF). Textural components (i.e., micropaleontological and sedimentological) are described and classified according to Dunham (1962) revised by Embry & Klovan (1971) and Folk (1959; 1962). Interpretations related to the depositional environments based on the parameters described in Wilson (1975) that he considered as Facies Zone (FZ) and as Standard Microfacies Zones (SMF) by Flügel (2010) are reported in Table 2. Thin sections were made at Estación Regional del Noroeste (IGL, UNAM) and Facultad de Ciencias de la Tierra (FCT-UANL).

Conodont extraction

The collected samples were processed following a modified version of the standard procedure published by Stone (1987) at the Laboratory of Conodonts (ConoLAB), Estación Regional del Noroeste (IGL, UNAM). Rock samples were fragmented, weighed, and placed in containers for disaggregation using a formic acid solution. The resulting insoluble residue was washed and sieved. The portion of the residue between 0.6 and 0.125 mm was then air-dried. The separation of conodont elements was carried out by hand-picking techniques with a binocular microscope. Conodont illustrations were taken with a TM3030 Plus Scanning Electron Microscope (SEM) located at the Estación Regional del Noroeste (IGL, UNAM). The conodont specimens are deposited in the collection of Paleontology of the Estación Regional del Noroeste (IGL, UNAM). Repository numbers are included in the plate captions.

RESULTS

Field observations

The Del Monte Formation includes Pennsylvanian strata from outcrops in both La Peregrina and Caballeros canyons but is more widely distributed in the Santa Ana River (Fig. 1). Local faults and deformation are common. These rocks are separated by unconformities from the Precambrian, Mississippian, and Permian strata. In this paper, based on the stratigraphic relation described by Stewart et al. (1999a) and our observations about the different exposition of conglomerates, sandstone, shale, and bioclastic beds, we subdivide the formation into the three following units.

Unit 1. Unit 1 is widely exposed in both La Peregrina (S1), and Caballeros canyons (sections S2, S3; S4; Fig. 3). In the La Peregrina Canyon Unit 1 is in contact with the Mississippian Aserradero Rhyolite (Fig. 2A). Its thickness varies from thick to medium on average with sub-vertical to horizontal beds; it also can contain wavy and irregular planes with lamination (Fig. 2B) and includes alternations of coarse- to medium-grained sandstone, calcareous sandstone, shale, calcarenite, bioclastic (fusulinid and ooidal fragments) grainstone, wackestone, mudstone, thin-conglomeratic beds and dolomitic limestone (Fig. 2C). Massive strata are less common, but preserve ammonoid molds (Fig. 2D). On the sandy and calcarenite beds, slumping and grading are common, even the trail segment of organisms can be preserved in several levels (e.g., Fig. 2D).

Unit 2. Although the base of Unit 2 is not exposed, the thickness is 30 m, measured to ~1 km east of El Naranjal Rancho along the Santa Ana River in the Caballeros Canyon and it is in contact with the Permian Guacamaya Formation. Unit 2 may also occur in La Peregrina Canyon, but it is in contact with Unit 1. Massive outcrops and thick-bedded strata characterize the unit, with occasional graded bedding, composed of conglomerate and breccia that contain abundant fine- to coarse-grained quartz and large mud fragments (< 10 cm; Fig. 2E). This unit differs from that referred to as the Naranjal Conglomerate (Ramírez-Ramírez 1992; Stewart et al. 1999a; Fig. 1B; Fig. 2G-H), in that it is light gray in weathered surface, with primarily angular to sub-angular components embedded in the cal-

careous matrix, although it may also contain some detrital fragments in thin-section (Casas-Peña et al. 2021). In contrast, the Naranjal Conglomerate has reddish tones, with clasts >20 cm derived primarily from igneous and metamorphic rocks (Fig. 2G-H).

Unit 3. Unit 3 represents the youngest unit of the Del Monte Formation and only includes at most a thickness of ~15 m. Unit 3 is characterized commonly by medium- to thin- and thick-bedded that interlayer gray-sandstone, siltstone and thin dark shale beds (Fig. 2F) and to a lesser extent, massive deformed black shale. Occasionally, the shale contains abundant organic matter. This unit can only be observed in stratigraphic section 3 (S3; Fig. 3) as a locally scattered part.

Conodont biostratigraphy

Three sections with a total of 12 samples were measured, six of which contained conodonts. A fourth section was studied, where a single sample was analyzed but no conodonts were recognized. Six genera (*Idiognathoides*, *Neognathodus*, *Idiognathodus*, *Streptognathodus*, *Adetognathus* and *Diplognathodus*), and several chondrichthyan ichthyoliths were identified in grainstone and dolomitic limestone of the Del Monte Formation (Table 1). Conodont associations indicate a biostratigraphic age that ranges from the Morrowan to the Atokan.

Section 1 (S1), Peregrina Canyon (~60 m). Three samples were collected, one from the basal level and two from the upper beds of the section (Fig. 2 and Fig. 3). Conodonts in the lowermost level (sample DM2-01), close to the contact with the Aserradero Rhyolite were absent. Still, several meters upwards of the Cuchilla Del Monte path, two bioclastic grainstone beds (samples DM2-02A and DM2-02B) contain P₁ and S conodont elements (Table 1), which allowed us to identify the Morrowan/Atokan boundary. In the uppermost sample of the S1 (DM2-02B), elements of the genera *Idiognathoides*, *Neognathodus*, *Idiognathodus*, and *Streptognathodus* were recognized, in addition to a single element of *Adetognathus* (Pl. 1 and Pl. 2).

In sample DM2-02A, species such as *Adetognathus lautus* (Gunnell, 1933), *Idiognathoides* cf. *Id. corrugatus* Harris & Hollingsworth, 1933, *Idiognathoides sulcatus sulcatus* Higgins & Bouckaert, 1968, *Idiognathoides convexus* (Ellison & Graves, 1941), *Streptogna-*

thodus parvus Dunn, 1966, and a few poorly preserved elements classified here as undeterminable species of *Idiognathoides*, *Idiognathodus*, and *Streptognathodus*, were identified (Table 1).

The sample DM2-02B, similar to the subjacent strata, includes specimens of *Idiognathoides* cf. *Id. corrugatus*, *Idiognathoides sulcatus sulcatus*, *Streptognathodus parvus*, as well as *Neognathodus* cf. *N. atokaensis* Grayson, 1984 and *Neognathodus atokaensis sensu* Lucas et al. (2017). Also, there are juvenile, broken or poorly preserved elements of undifferentiated species of *Streptognathodus*.

Thus the Morrowan/Atokan boundary can be located in this canyon, between samples DM2-02A and DM2-02B.

Section 2 (S2), Caballeros Canyon. Five samples were collected from different horizons in Section 2, four carbonate and one clastic. Only three samples contained conodonts (Fig. 3). The most abundant genera are *Idiognathoides* and *Idiognathodus*, with rare occurrence of *Neognathodus*. Species of the genera *Diplognathodus* and *Streptognathodus* were also found. As in S1, the Morrowan/Atokan boundary was identified.

The lower part of the S2 is characterized by species that also occur in the La Peregrina Canyon, such as *Idiognathoides* cf. *Id. corrugatus*, *Id. sulcatus sulcatus*, *Id. convexus*, as well as *Idiognathoides asiaticus*

Fig. 2 - Outcrops of the Pennsylvanian Del Monte Formation, Tamatán Group. A) La Peregrina Canyon, above Cuchilla del Monte path; In Section 1 (S1), the contact between Mississippian Aserradero Rhyolite and the base of the massive Pennsylvanian strata of Unit 1 of the Del Monte Formation can be recognized (black dashed line). B) Caballeros Canyon, Unit 1; the lower part - Section 2 (S2) consists of medium thickness, wavy-bed of calcarenite with parallel lamination, C) Caballeros Canyon, upper part - Section 2 (S2) includes upward graded succession of thin to thick limestone layers, D) Caballeros Canyon, lower part - section 3 (S3) comprises medium thickness of calcarenite/grainstone intercalated with laminated siltstone. Note: the red arrow shows the trail segment of the fossil, and the blue arrow exhibits the ammonoid mold (goniatites?). E) Caballeros Canyon, Section 4 (S4) the conglomeratic calclithite massive strata with subrounded rip-up mud clasts of Unit 2, and F) the upper part - Section 3 (S3) thin intercalation of calcareous sandstone and shale beds of Unit 3. G-H) Caballeros Canyon, Naranjal conglomerate outcrops include mostly igneous fragments up to ~20 cm, location is referred in Fig. 1.



FIGURE 2

Local stratigraphic sections (measure)	S1 (~ 60 m)			S2 (~ 60 m)					S3 (~ 15 m)				S4 (~ 25 m)
Species (P ₁ and S elements) / Samples	DM2- 01	DM2- 02A	DM2- 02B	CC54- 12	CC54- 11	CC54- 10	CC54- 09	CC54- 08	CC54- 07	CC54- 06	CC54- 05	CC54- 04	CC44-03
<i>Adetognathus lautus</i>		1											
<i>Diplognathodus coloradoensis</i>				6	1								
<i>Idiognathoides corrugatus</i>										1			
<i>Id. cf. Id. corrugatus</i>		1	1					1					
<i>Id. sulcatus sulcatus</i>		1	1	3									
<i>Id. convexus</i>		1		2									
<i>Id. asiaticus</i>				3	1			2					
<i>Id. sp. (und.)</i>		1		2	1			8					
<i>Neognathodus atokaensis</i>			1					1					
<i>N. atokaensis sensu</i> Lucas et al. 2017			1					1					
<i>N. aff. bothrops</i>								2					
<i>N. sp. (und.)</i>			1	2	3			1	3				
<i>N. cf. N. expansus</i>								1					
<i>N. nataliae</i>								1	2				
<i>Idiognathodus aff. I. delicatus</i>				2				14	5				
<i>I. incurvus</i>								2	7				
<i>I. sp A</i> Grubbs 1984				2									
<i>I. n. sp B</i>									1				
<i>I. n. sp C</i> (gerontic)									1				
<i>I. n. sp. D</i> (gerontic)									1				
<i>I. sp. (und.)</i>		1		1	1			5	4				
<i>Streptognathodus parvus</i>		1	1										
<i>St. sp. (und.)</i>			1					1	4				
Ramiform elements (S)	15	10		60	35			124	12				
Total	22	17		83	42			150	40				
Total amount dissolved	1.243	2.417	2.332	0.545	0.271	0.004	0.21	0.305	0.319	0.395	0.072	0.055	0.266
Conodonts/kg	0	9	7	152	155	0	0	492	0	53	0	0	0
Ichthyoliths		7	8	27	11			37	18				
% in Genera (Sum = 100 %)													
<i>Adetognathus</i> (%)		5	-	-	-			-	-				
<i>Diplognathodus</i> (%)		-	-	7	2			-	-				
<i>Idiognathoides</i> (%)		18	12	12	5			7	2				
<i>Neognathodus</i> (%)		0	18	2	7			5	12				
<i>Idiognathodus</i> (%)		5	-	6	2			14	46				
<i>Streptognathodus</i> (%)		5	12	-	-			1	10				
Ramiform (%)		68	59	72	83			73	29				0

Tab. 1 - Conodont abundance data for the Del Monte Formation, NE de Mexico.

Nigmatganov & Nemyrovskaya, 1992. In addition, two P₁ elements of *Idiognathodus* sp. A Grubbs, 1984 were identified in level CC54-12. *Diplognathodus col-*

oradoensis (Murray & Chronic, 1965) was found in both levels, as well as several poorly preserved *Idiognathoides* sp.

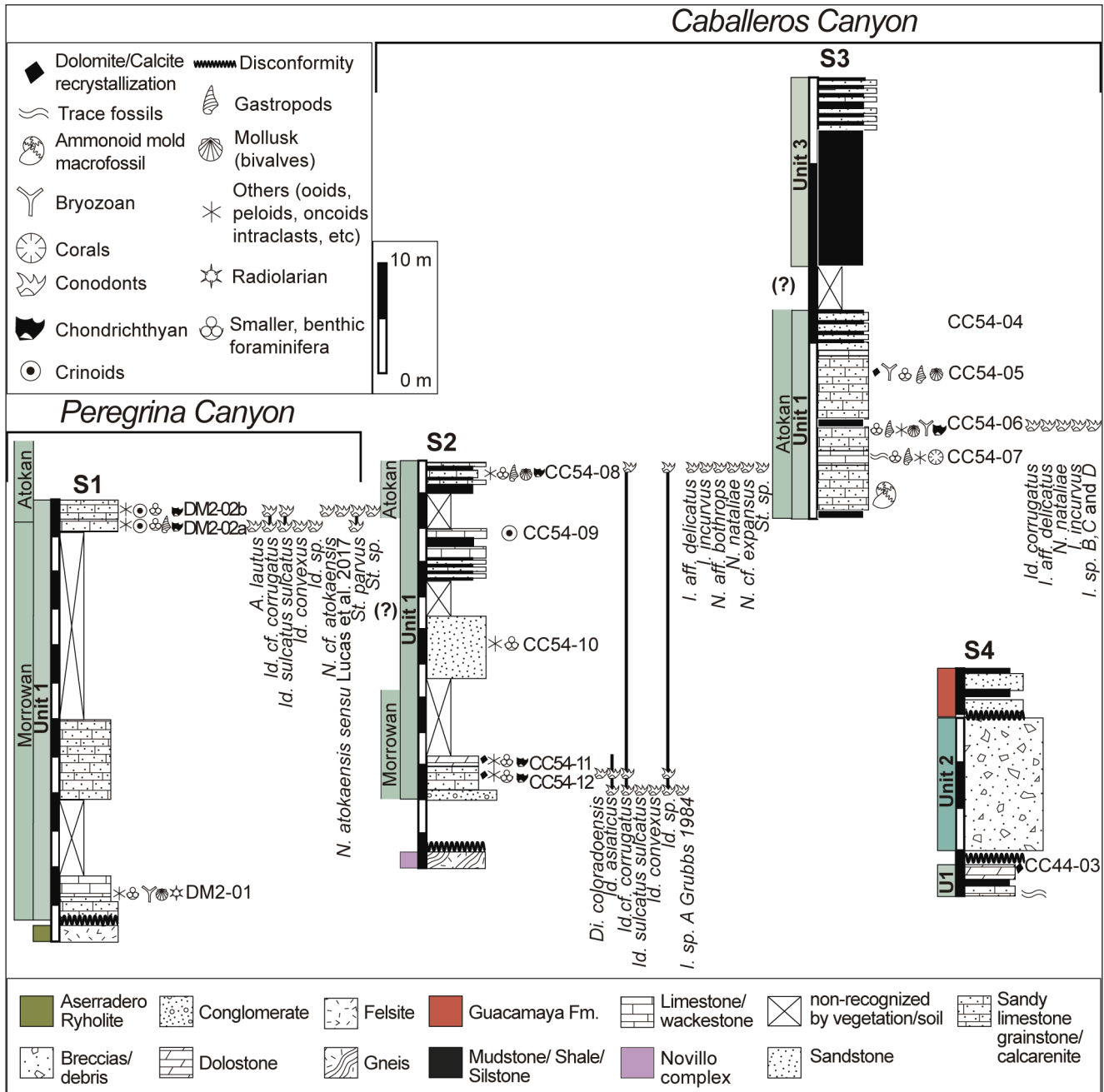


Fig. 3 - Stratigraphic sections, sample locations, and conodont distribution from the Del Monte Formation strata exposed in the La Peregrina and Caballeros canyons in the Huizachal-Peregrina Anticlinorium and sample positions. Note: Stratigraphic sections (S1 – S4) are located in the geological map in Fig. 1B.

Conodonts were not found in the clastic and carbonate beds from the middle part of section 2. However, the upper beds of this section, especially level CC54-08, exhibit a notable abundance of fragments of ramiform (S) and P₁ elements, compared to the other samples (see Table 1). The fossil assemblage found in level CC54-08 includes species such as *Idiognathoides* cf. *Id. corrugatus*, *Idiognathodus* aff. *delicatus* Gunnell, 1931, *Idiognathodus incurvus* Dunn, 1966, *Neognathodus* aff. *bothrops* Merrill, 1972,

Neognathodus nataliae Alekseev & Gerelzezeg, 2001 (in Alekseev & Goreva 2001), *Neognathodus* cf. *Neognathodus expansus* (Jones, 1941), as well as several undeterminable specimens of *Idiognathodus*, *Idiognathoides* and *Streptognathodus*.

Section 3 (S3), Caballeros Canyon. Four samples were collected in Unit 1, but only one contained conodonts. In this sample, we identified a conodont association corresponding to the early to middle

Atokan. This association is mainly represented by *Idiognathoides corrugatus*, *Idiognathodus* aff. *delicatus*, *I. incurvus*, *N. nataliae*, and a few specimens of the genus *Idiognathodus*. These specimens of *Idiognathodus* are herein defined as *Idiognathodus* sp. B, and gerontic specimens as *Idiognathodus* sp. C, and *Idiognathodus* sp. D (Plate 2; Table 1), due to their particular characteristics such as large and elongate platforms with a carina dorsally extended (up to $\frac{3}{4}$ of the platform) and few transversal ridges with a sub-rounded dorsal tip, robust platforms with the accessory lobes and carina fused in the ventral part and abundant transversal ridges with a dorsally pointed tip.

Section 4 (S4), Caballeros Canyon. The S4 contains sandstone, siltstone, dolomitized limestone of Unit 1, and massive detrital flow-type conglomeratic beds of Unit 2 that are subjacent discordantly to the Guacamaya Formation. A sample of the dolomitized limestone was collected in this section, but no conodonts were recovered.

Microfacies

The distinct microfacies of the Del Monte Formation were identified as (MF1) bioclastic grainstone, (MF2) bioclastic wackestone, (MF3) dolomite sparstone or dolostone, (MF4) laminated mudstone, and (MF5) siliciclastic sandstone. Table 2 summarizes the recognized features. The skeletal grains can include benthic foraminifera, gastropods, mollusk fragments, bivalves, and radiolarians. Non-skeletal grains include coated grains such as ooids, peloids, and intraclasts, and detrital grains such as monocrystalline quartz, feldspars, and micas. The groundmass of the sampled rocks usually consists of calcite sparite cement, which occasionally recrystallizes to dolomite and/or alternates to micrite.

MF1 Bioclastic grainstone. Grainstone is the most common microfacies of Unit 1 of the Del Monte Formation, and is represented by samples DM2-02A and DM2-02B from La Peregrina Canyon (S1) and CC54-12, CC54-08, CC54-06 from Caballeros Canyon (S2), respectively (Fig. 4; Fig. 5). Two sub-microfacies are distinguished based on the dominant allochems (skeletal grains) which usually are embedded in sparite groundmass. Smf1: The grainstone with coated grains and peloids (bio-oosparite sensu Folk 1959; Fig. 4C-F), dominates in samples DM2-02A and DM2-02B, formed mainly

by ooids, micritic intraclasts, peloids, and subsequently bioclasts. A large amount of rounded to elliptical concentric ooids are packed by sparite and micritic nucleus and a cortex whose thickness is one or two laminae (e.g., Fig. 4 C-D). The sub-rounded intraclasts are usually of micrite or contain detrital or bioclastic micro-fragments. Peloids are rounded, elliptical, or oval-shaped and composed of structureless microcrystalline carbonate. The bioclasts are benthic foraminifera that include *Climacamina* sp. and *Fusulina* sp.? (Fig. 4 C-F), mollusk and bivalve shell fragments, echinoderms, and bryozoans. The other sub-microfeature (Smf2) consists of bioclastic grainstone (biosparite; Fig. 5 C, E) and is reflected in samples CC54-12, CC54-08 and CC54-06, which contain mainly skeletal grains of benthic foraminifera such as *Millerella* sp., also broken fragments of gastropods as well as large bivalves occur (Fig. 5C). Consequently bryozoans and echinoderms can occasionally be covered by syntaxial calcite cement. Irregular peloids, micritic intraclasts, and oncoids are subordinate. Although both sub-microfeatures groups can be evaluated as bioclastic grainstone, the frequency of coated grains is more remarkable in the first subgroup of samples than in the second. It also has detrital grains with sub-angular and sub-rounded quartz, feldspar, and micas.

Fig. 4 - Photomicrographs of the microfacies from the calcareous rocks of the Del Monte Formation, in the La Peregrina and Caballeros canyons. Most photos are under parallel Nicols (NII) (x 2.5). White bar represents 1 mm. A-B) Bioclastic wackestone (biomicrite) including bryozoa (bri) associated with micritic micro fenestrae (fe), echinoderm (ec), mollusk fragment (ml) and radiolaria (r) embedded in micritic matrix with oxides stylolites, sample DM2-01. C-D) Bioclastic grainstone with benthic foraminifera (fo) such as *Climacamina* sp.? (cli), *Millerella* sp. (mil), abundant micritic coated grains such as ooids (o), peloids (pe), reworked intraclasts (in) and stylolites with Fe, sample DM2-02A. E-F) Bioclastic grainstone (bio-oosparite) with foraminifera (fo) *Fusulina* sp. (fu), bivalves (bi), gastropods (ga), echinoderm (ec), intraclasts (In) and abundant ooids (oo) embedded in sparitic cement also calcite veins (ca) occur, sample DM2-02B. G) Bioclastic grainstone (biosparite) with foraminifera (fo), crinoids (cr), ooids (oo), and micritic peloids (pe) embedded in sparite cement; also thin calcite veins occur, sample CC54-12. H) Dolostone partially covered with inequigranular texture and porphyrotopic fabric. Micritic groundmass (red arrow) and the dolomite replaced (do) and calcitic veins (ca) occur, sample CC54-11.

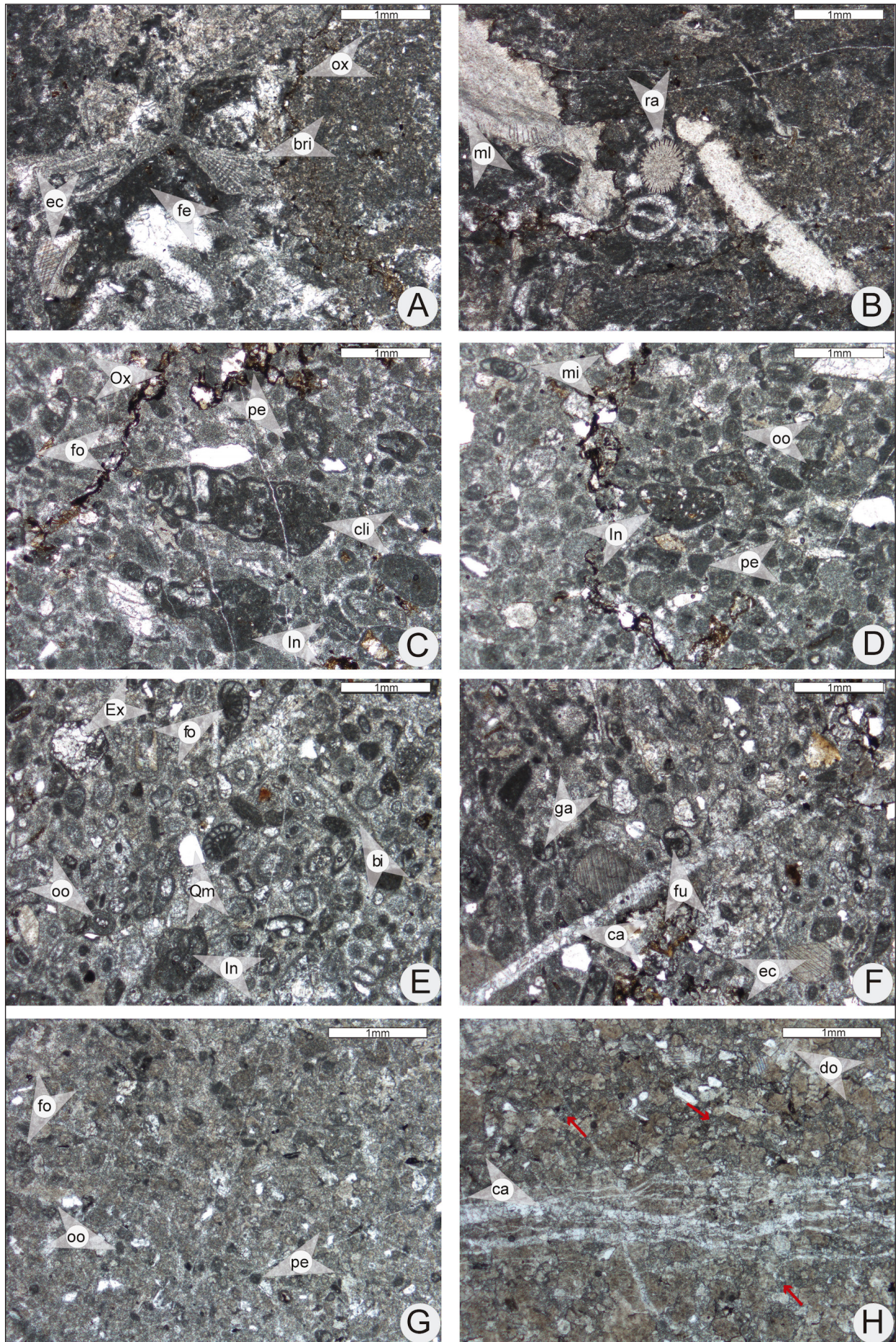


FIGURE 4

Locally neomorphism of mosaic-like dolomite or calcite patches may occur (e.g., Fig. 5C). Fe-oxides can occur as opaque fragments (i.e., pyrite, hematite) or appear dissolved in stylolites and fractures; also calcite veins are present.

MF2 Bioclastic wackestone. Wackestone (biomicrite *sensu* Folk 1959) is subordinate of Unit 1 in the Del Monte Formation, including the samples DM2-01 (La Peregrina Canyon; S1), CC54-09, CC54-07 and CC54-05 (Caballeros Canyon; S2 and S3; Fig. 3). The sample DM2-01 preserves more variability of microfossils such as benthic foraminifers, bivalves, radiolarians, corals and bryozoans (e.g., Fig. 4 A, B). Most fossil assemblages in the other samples contain coated reworked micritic intraclasts, bioclasts (Fig. 5D), and in less proportion, echinoderms, and ooids, while quartz grains can be frequent (Table 2). Several grains show recrystallization as calcite overgrowth rims (e.g., Fig. 5F). The micritic groundmass is commonly accompanied by Fe-oxides such as pyrite, hematite, even oxides-fill stylolites and probably fenestrae development can occur (Fig. 4A; sample DM2-01).

MF3 Dolomitic limestone. The dolomitic limestone or dolostone (dolomicrite) is less common but can occur in several horizons of the Del Monte Formation such as the samples CC54-11 and CC44-03. The samples are formed mainly of inequigranular texture with non-rhombic dolomite; although may occur as a tightly packed anhedral and subhedral as hypidiotopic fabric ranging from 10 to 200 μm in size (Fig. 4H, Fig. 5H). The intergranular boundaries may be lobate or straight with some punctual junctions. A hand sample typically shows pale orange, pink-orange weathering tones, and light orange-gray in fracture. This layer is apparently related to wackestone, due to the framework is mostly composed of fractured detrital quartz grains, and subordinately bioclastic grains such as very small foraminifers and coated grains like peloids, which are very difficult to identify due to their complete dolomitization, but partially covered grains also can occur. The groundmass is of micrite (Fig. 4H, Fig. 5H).

MF4 Mudstone. Sample CC54-04 preserves a dusky yellow- to olive-black color in hand-sample. The thin section corresponds to a mudstone (or

micrite), characterized by the presence of silt-sized quartz and lime mud (Fig. 5G). This microfacies often exhibits a laminated structure. Notably, it lacks bioclasts, but few relicts of micritic intraclasts and opaque minerals can be observed.

MF5 Siliciclastic sandstone. In the Del Monte Formation, fine- to coarse-grained sandstone with moderate to poor sorting intercalate the bioclastic calcareous successions in Unit 1. Sample CC54-10 represents a medium-grained sandstone poorly sorted. Detrital grains are predominantly monocrystalline quartz, more abundant than polycrystalline quartz, feldspar, mainly potassium microcline and plagioclase, with less orthoclase and mica, such as muscovite. Bioclasts of foraminifera *Fusulina* sp. (?) and limestone lithics also occur; chert is rare. Accessory grains such as zircons that occasionally

Fig. 5 - Photomicrographs of the microfacies from the calcareous and calcareous rocks of the Del Monte Formation, in the Caballeros Canyon. Most photos are under parallel Nicols (NII) (x 2.5). White bar represents 1 mm. A) Medium-grained sandstone consists of subrounded monocrystalline (Qm) and polycrystalline quartz (Qp), feldspar (Ksp), muscovite (Mo), and *Fusulina* sp.? (fo) and calcite grains (Lc) embedded in calcite cement (crossed nicols). The filling of the grain cracks by clay (red arrow), calcite overgrowths in the grains (blue arrow), and hematite grains (yellow arrow) occur, sample CC54-10. B) Bioclastic wackestone (biomicrite) consists of indeterminate bivalves (bi), a large number of ooids (oo) with calcite and micritic nuclei, detrital and pyrite grains (ox) embedded in micritic matrix replaced with calcite patch (blue arrow), also stylolites filled with Fe-oxides and calcite appear, sample CC54-09. C) Bioclastic grainstone (biosparite) with foraminifers (fo), gasteropods (ga), and bivalves (bi), sub-rounded detrital grains and hematites (ox) embedded in sparite groundmass (red arrow) partially replaced with calcite cement which occasionally appears like patches (blue arrow), sample CC54-08. D) Wackestone (biomicrite) with large micritic grain-aggregate intraclasts (In), echinoderm (ec) embedded in a micritic matrix. Sample CC54-07. E) Bioclastic grainstone (biosparite) with foraminifers (fo), fenestrate? bryozoans (br), oncoids (oc), and hematite oxides (ox), sample CC54-06. F) Wackestone (biomicrite) containing bryozoan (br), limestone lithoclasts (ca) with recrystallized calcite overgrowth rim (blue arrow), and detrital grains (Qm). Sample CC54-05. G) Laminar mudstone (laminated micrite) with detrital elongate to subrounded grains, micritic intraclast relict-like (blue arrows), and opaque grains, sample CC54-04. H) Dolomitic limestone micritic groundmass (red arrow) replaced by inequigranular dolomite texture with porphyrotopic fabric (blue arrow), preserving a mollusk? fragment (ml), intergranular oxides (ox), detrital grains (Qm), sample CC44-03.

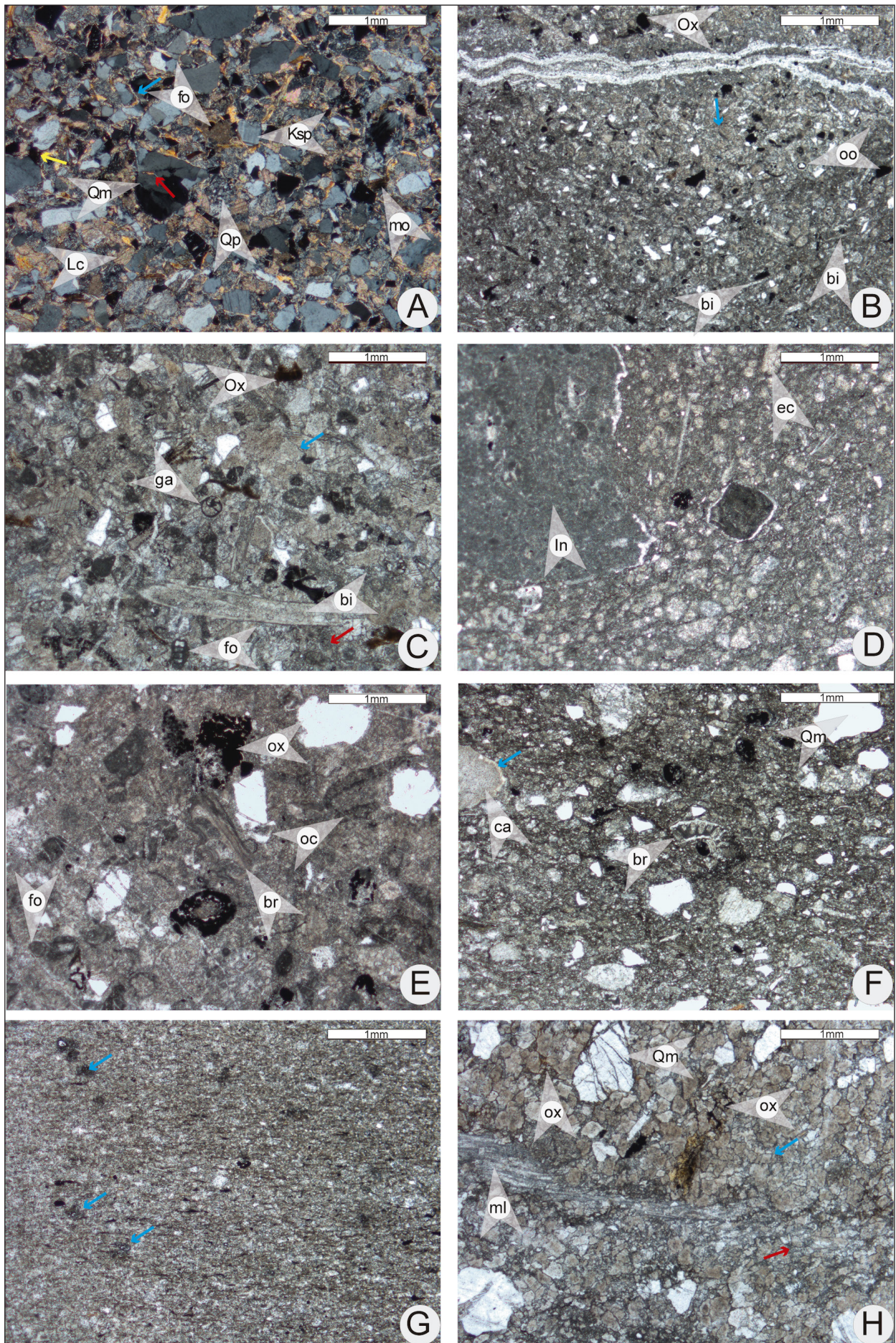


FIGURE 5

incrusted on quartz grains, and opaque grains (e.g., pyrite, hematite) occur. The framework grains are embedded in calcite/sparite cement which may replace detrital grains or fill grain cracks (Fig. 5A). In Casas-Peña et al. (2021) an exhaustive review of the composition and provenance of the siliciclastic horizons of the Del Monte Formation is included.

DISCUSSION

Biostratigraphic considerations

Three sections across the Del Monte Formation in the Tamatán Group (Tamaulipas, NE Mexico) were herein measured and sampled for conodont studies. We obtained six different conodont associations which indicate Morrowan and Atokan ages. Specifically, S1 (Peregrina Canyon) and S2 (Caballeros Canyon) include Morrowan conodonts in the lower part, and Atokan conodonts in the upper interval. These occurrences allow the identification of the Morrowan/Atokan boundary in both Peregrina and Caballeros Canyons. In S3, all conodonts found indicate an Atokan age.

In several studies of Lower to Middle Pennsylvanian conodonts (e.g., Ellison 1941; Dunn 1970a; Lane et al. 1970; Lane & Straka 1974; Nemyrovskaya 1999; Fohrer et al. 2007; Nemyrovskaya et al. 2011; Sungatullina 2014; Qi et al. 2015; Hu et al. 2016; Cardoso et al. 2017a; Barrick et al. 2013), and as our assemblages, the coexistence and grouping of morphotypes in one or more stratigraphic levels ranging from the Morrowan to the Atokan are commonly documented in several localities of North America, South America as well as from the Bashkirian to the Moscovian in Europe. For example, Dunn (1970a; 1970b) reports that the Bird Spring and Ely Limestone formations in Nevada, Round Valley Formation in Utah, and Bloyd Formation in Oklahoma include the coexistence of *Adetognathus lautus*, *Idiognathoides convexus* and *Streptognathodus parvus* within the *Streptognathodus parvus* – *Adetognathus spathus* Zone, which indicates a middle-upper Morrowan age. The coexistence of *Adetognathus lautus* and *Streptognathodus parvus* can also be recognized in the Itaituba Formation from the Tapajos Group in the Amazonia Basin (Cardoso et al. 2017a). On the other hand, *Idiognathodus corrugatus* and *Id. sulcatus sulcatus* appear in the Mandrykinsky and Kayalsky horizons of Bashkirian (Morrowan) in the Donetsk Basin

(Nemyrovskaya 1999). This faunal association and other morphotypes have also been documented at the Bashkirian/Moscovian boundaries of the Naqing and Luokun sections in South China (Qi et al. 2015; Hu et al. 2016). Herein, the Morrowan and Atokan ages are recognized for northeastern Mexico, as the different species in the localities mentioned above can be found grouped in the level DM2-02A, which indicates a Morrowan age. Conversely, the occurrence of *Neognathodus* cf. *atokaensis* and *N. atokaensis sensu* Lucas et al. (2017) in the overlying strata DM2-02B indicates a younger age corresponding to the Atokan (Sungatullina 2014; Qi et al. 2015).

In the S2 from the Caballeros Canyon, the conodont assemblages from the two lowermost beds indicate a late Morrowan age. Studies reporting *Idiognathoides corrugatus* and *Id. sulcatus sulcatus* in uppermost Morrowan and lowermost Atokan strata include the works of Sungatullina (2014) and Hu et al. (2016). It should be noted that *Idiognathodus* sp. A Grubbs 1984 from level CC54-12 is a morphotype that only differs from *Idiognathodus* sp. A Grubbs 1984 reported in Nemyrovskaya (1999), in having a narrower platform; however, our specimens are similar to *Idiognathodus* sp. A in having a nodular carina that extends towards the dorsal part, a diagnostic character for the species (Grubbs 1984). Similarly, the P₁ elements described by Grubbs (1984) have curved platforms with a free blade that joins in the middle of the platform and they are ornamented by well-developed accessory lobes and transverse ridges. One of our specimens perfectly matches the morphotype described by Grubbs (1984), while other preserves only the long, smooth carina without the development of accessory lobes (see Pl. 1-14 and 15). *Idiognathodus* sp. A Grubbs (1984) has been reported in the upper part of the Wapanucka Formation and it is widespread in the Atokan Formation in North America (Grubbs 1984), and the Itaituba Formation in South America (Cardoso et al. 2017b), at the Bashkirian/Moscovian boundary in the Naqing section of southern China (Qi et al. 2015), and in the Bashkirian and Moscovian beds of the Karaguz Valley section in the Donetsk Basin (Nemyrovskaya 1999). The age range of this morphotype extends from the late Morrowan to the early Atokan. On the other hand, Hu et al. (2016) reported an association of conodonts with the occurrence of *Idiognathoides corrugatus* and *Diplognathodus coloradoensis* in several beds of the uppermost Bashkirian and lowermost Moscovian in the Luokun sec-

tion of southern China, indicating a late Morrowan or early Atokan age.

The middle part of S2 is barren in conodonts, making it difficult to determine whether the Morrowan continues or if it is already the Atokan. Meanwhile, the fossil assemblage recognized in the upper part of the S2, according to the sample CC54-08 (see Conodont biostratigraphy section above), as well as the extensive record of *Idiognathoides*, *Idiognathobodus* and to a lesser extent, *Neognathobodus*, in North America (e.g. Thompson & Lambert 2017; Barrick et al. 2022), South America (e.g. Cardoso et al. 2017a), Ukraine (e.g. Nemyrovska 1999), and Russia (e.g. Sungatullina 2014) allow us to infer an Atokan age.

On the other hand, sporadic reports of *Neognathobodus expansus* (Jones, 1941) indicate a more restricted occurrence in the Midcontinent Basin, particularly in the Homer School Limestone in Kansas and Oklahoma and/or the Lost Branch Formation (Rosscoe 2005). It has also been documented in the Gobbler Formation in the Sacramento Mountains, New Mexico (Lucas et al. 2021). The age range of this morphotype, together with other species including *Neognathobodus dilatatus dilatatus* (Stauffer & Plummer, 1932) and *Hindeodus minutus* (Ellison, 1941), corresponds to a Desmoinesian age. However, compared to the Midcontinent Basin specimens, our specimens appear together with Atokan species.

In the S3, only the sample CC54-06 contains a conodont association. According to our observations, this layer yield similar conodont assemblages to the upper part of section 2 which can also indicate an early to middle Atokan age. In addition, the conodont bed CC54-06 overlies a bed containing an ammonoid mold described by Murray et al. (1960) as *Eoasianites* sp., together with fusulinids such as *Fusulinella* sp., therefore confirming an Atokan age.

We conclude that the productive strata of S1 and S2 suggest an age ranging from Morrowan to Atokan. In contrast, the productive conodont-bearing strata in S3, which are close to the bed with the ammonoid mold described by Murray et al. (1960), points to an Atokan age. The Desmoinesian age proposed by Stewart et al. (1999a) remains uncertain, as it could not be definitively confirmed. This uncertainty arises from the wide stratigraphic range of species such as *Idiognathobodus delicatus*, spanning from the Atokan to the Missourian, which was probably the basis for assigning the proposed Desmoinesian age.

Rosscoe & Barrick (2009) comprehensively detailed morphological variations of *Idiognathobodus* in successions from the Desmoinesian to Missourian cyclothems in the Midcontinent Basin of North America. Unfortunately, these morphotypes are not recognized in the beds examined in our study. Although the Atokan/Desmoinesian boundary could perhaps be located along the S3, where only Atokan conodont elements were identified, more thorough and systematic sampling based on the explored and examined strata is needed to refine the conodont biostratigraphy.

Depositional environment

The combination of field observations, conodont analyses, and microfeatures of the calcareous rocks described above provides a comprehensive understanding of the potential facies zones (FZ) and depositional environment of Pennsylvanian carbonate rocks in the Tamatán Basin. It is evident from our study that the calcareous beds of Unit 1 represent shallow-water marine platform sediments. Additionally, other facies and deposits identified here as Unit 2 and Unit 3 from the Del Monte Formation are related to slope and even deeper marine environments, as reported previously by other authors (e.g., Murray et al. 1960; Carrillo-Bravo 1961; Ramírez-Ramírez 1992; Stewart et al. 1999a).

Field observations in Unit 1 reveal predominantly thick to medium bedding in several stratigraphic levels, comprising dolostone, laminated limestone, grainstone, and less frequently, thin calcarenite and conglomeratic beds. Most of the calcareous beds, as suggested by microfacies analyses, indicate a shallow marine environment associated with the platform margin. On the other hand, sandy levels, often preserving sedimentary structures such as wavy horizons, grading, and slump structures, imply that the sandy-calcareous successions were influenced by a slope where sediments could potentially slide downslope.

The microfacies analysis of Unit 1 (Table 2a,b) reveals two distinct depositional environments within the shallow-marine platform. The first environment is linked to a platform margin characterized by sandbars, shoals, or winnowed sands. The second environment is associated with an interior platform, indicating a more restricted shallow basin (Fig. 6).

Sedimentological features	Sample	Rock color in weathering / fracture	Latitude / Longitude	Microfeatures	Framework grains				Facies zone
					skeletal	non-skeletal	detrital	others	
La Peregrina canyon: S1 (~60 m)									
Mostly, bioclastic limestone and calcarenite.	DM2-01	yellowish-gray / light gray	23°46'33"/99°15'56"	MF2: bioclastic wackestone (biomicrite) with micritic matrix and micro-fenestrae development (SMF: 8, 9)	Bryozoan, echinoderm, benthic foraminifera, gastropod, mollusk, radiolarian	Intraclasts, ooids, peloids	Quartz	Oxides, stylolite, calcite veins	Open Marine (7)
Thickness from massive to medium beds range from 60-30 cm.	DM2-02a*	brown-gray / dark gray	23°46'33"/99°15'56"	MF1: ooidal grainstone (bio-oosparite), abundant coated grains and fewer bioclasts (SMF: 11)	Bryozoan, benthic foraminifera, gastropod	Intraclasts, ooids, peloids	Quartz, micas	Oxides, stylolite, calcite veins	Platform margin (6 and/or 5)
Commonly calcite veins	DM2-02b*	brown-gray / dark gray	23°46'33"/99°15'56"	MF1: ooidal grainstone (bio-oosparite), abundant coated grains and less bioclasts (SMF: 11)	benthic foraminifera, gastropod	Intraclasts, peloids	Quartz	Micro-stylolite, calcite veins	Platform margin (6 and/or 5)
Caballeros canyon: S2 (~60 m)									
Mostly, bioclastic limestone, dolostone, sandstone and shales intercalated. Structureless massive and to thick and medium average (40 - 20 cm).	CC54-12*	orange-pink / grayish blue	23°48'28"/99°17'27"	MF1: bioclastic grainstones (biosparite), micro-spar (SMF: 11)	Undifferentiated bivalve, benthic foraminifera	Ooids	Quartz	Oxides, micro-stylolite, calcite veins	Platform margin (6 and/or 5)
	CC54-11*	very pale orange / light-olive gray	23°48'28"/99°17'27"	MF3: Recrystallized dolomite / dolostone (dolomicrite) with micritic groundmass and dolomite patches (SMF: 19 or 23)	benthic foraminifera	Relict ooids?	Quartz	Oxides, micro-stylolite, calcite veins	Platform interior (8)
	CC54-10	pinkish gray / medium gray	23°48'31"/99°17'24"	MF5: Quartz-feldspathic sandstone	benthic foraminifera	Intraclasts	Quartz, feldspar, micas	oxides	Platform margin related with sand bars (6)
	CC54-09	pinkish gray / medium gray	23°48'34"/99°17'23"	MF2: bioclastic wackestone (biomicrite), micrite matrix with calcite patches (SMF:9)	Undifferentiated bivalve	Ooids, peloids	Quartz	Oxides, micro-stylolite, calcite veins	Open Marine (7)
	CC54-08*	pale-brown / dark-gray	23°48'39"/99°17'25"	MF1: bioclastic grainstone (biosparite) cement with calcite patches (SMF: 11)	Undifferentiated bivalve, echinoderm, benthic foraminifera, gastropod, mollusk	Intraclasts, peloids	Quartz	Oxides	Platform margin (6 and/or 5)

Tab. 2a - Microfacies analysis of Unit 1 of the Del Monte Formation, NE de Mexico. Note: asterisk indicates the samples with conodont and SMF= standard microfacies zone.

The MF1 grainstone includes coated bioclasts and skeletal assemblage comprising foraminifera, bivalves, bryozoans, and echinoderms. These characteristics indicate the first depositional environment domain, corresponding to a platform-margin setting involving a FZ 6 even FZ 5 of Wilson (1975), and SMF 11 (Flügel 2010). This environment can be characterized by normal marine salinity above

the fairweather wave-base. Still, it can be influenced by marine currents with high energy due to abundant coated bioclasts (Fig. 6).

In contrast, paleoecological and biofacies models based on Pennsylvanian conodonts (Swade & Heckel 1985; Davis & Webster 1985; Heckel 1994; Brown et al. 2016; Cardoso et al. 2017a) are commonly associated with carbonate ramp mod-

Sedimentological features	Sample	Rock color in weathering / fracture	Latitude / Longitude	Microfeatures	Framework grains				Facies zone
					skeletal	non-skeletal	detrital	others	
Caballeros canyon: S3 and S4 (~15 and 25 m, respectively)									
Mostly, bioclastic limestone, dolostone, sandstone and shales. Thin beds less common. Bedding planes frequently are wavy and irregular, occasionally horizontal lamination or in ripples. Slump and sole marks are infrequent.	CC54-07	greenish gray / brownish black	23°48'48" / 99°17'20"	MF2: bioclastic wackestone (biomicrite), micrite matrix with calcite patches (SMF: 9)	Undifferentiated bivalve, echinoderm		Quartz, feldspar	Oxides, micro-stylolite, calcite veins	Open Marine (7)
	CC54-06*	brownish gray / light-gray	23°48'48" / 99°17'20"	MF1: bioclastic grainstone (biosparite) with calcite patches (SMF: 11)	Undifferentiated bivalve, bryozoan, echinoderm, benthic foraminifera, mollusk	Intraclasts, ooids	Quartz	Oxides, calcite veins	Platform margin (6 and/or 5)
	CC54-05	greenish gray / brownish black	23°48'48" / 99°17'20"	MF2: bioclastic wackestone (biomicrite) (SMF: 9)	Undifferentiated bivalve, bryozoan, coral, benthic foraminifera, mollusk	Intraclasts, ooids	Quartz, Micas	Oxides, micro-stylolite	Open Marine (7)
	CC54-04	dusky yellow / olive black	23°48'48" / 99°17'20"	MF4: Mudstone Laminated (laminated micrite) with moderate amount of fine detrital grains (SMF: 3 or 23)		Micritic intraclasts relicts?	Quartz, Micas	Oxides, calcite veins	Deep Shelf (3) or Platform interior (8)
	CC44-03	pink orange / orange-gray	23°49'7" / 99°17'8"	MF3: Recrystallized dolomite / dolostone (dolomicrite) (SMF: 19 or 23)		Intraclasts	Quartz, feldspar	Oxides, calcite veins	Platform interior (8)

Tab. 2b - Microfacies analysis of Unit 1 of the Del Monte Formation, NE de Mexico. Note: asterisk indicates the samples with conodont and SMF= standard microfacies zone.

els, and the genera *Neognathodus*, *Idiognathodus*, and *Streptognathodus* are found in calcarenites and calcilitites, mainly in environments where the wave base is conditioned by open seas with warm, oxygen-rich waters (e.g. Sweet 1988; Heckel 1994), features that may be similar to Unit 1 of the Del Monte Formation. Additionally, the carbonate ramp models also suggest that *Neognathodus* and *Adetognathus* appear in more restricted biofacies such as bars, lagoons, and/or tidal environments, as documented by Davis and Webster (1985) in the Alaska Bench Formation in Central Montana, United States. Brown et al. (2016) further discuss that conodonts are more abundant in limestones than in detrital beds (e.g., shales) and prefer relatively clastic-free open-marine environments. However, despite the limited number of the conodonts found in Unit 1 of the Del Monte Formation, they are predominantly present in the bioclastic grainstone microfacies, in which coated grains are also observed. The identification of al-

lochems, such as foraminifera (*Climacamina* sp.?, *Millerella* sp., *Fusulina* sp.), bivalves, and gastropods in the microfacies of Unit 1 as well as the consideration of sedimentary structures, and deeper facies of the Unit 2 and Unit 3 allow us to propose, in contrast to carbonate ramp models, a shallow platform margin model for Unit 1 which is associated with wave activity close to an open marine slope environment. Supporting evidence for a shallow environment in the Del Monte Formation includes the presence of bathymetric index fossils such as ammonoids (Malpica & De La Torre 1980).

Therefore, most conodonts of the Del Monte Formation are associated with the bioclastic grainstone (MF1) including genera *Idiognathoides*, *Neognathodus*, *Idiognathodus*, and *Streptognathodus*, and to a lesser extent, *Diplognathodus* and *Adetognathus*, and they are related to an open marine area (Fig. 6). Although *Adetognathus* and *Diplognathodus* are typically found in restricted environments, our specimens

have been identified in both settings—a quiet environment with developed dolomitization (e.g., level CC54-11) and on the platform margin (CC54-12).

Similar to MF1 but with bioclasts embedded in micritic cement, the wackestone of MF2 includes skeletal components such as benthic foraminifera, mollusks, bryozoans, gastropods, undifferentiated bivalves, and micritic intraclasts. These elements denote an open-marine fauna originating from a shallow platform circulation environment (FZ 7; Wilson 1975), corresponding to SMF 9 (Flügel 2010). Additionally, micro-stylolites with oxides in grainstone and wackestone likely served as fluid conductors during the diagenesis and compaction as documented by several authors (e.g. Vandeginste & John 2013; Gyori et al. 2020; Gomez-Rivas et al. 2022). The microfenestra fabric may also have formed during these processes. As discussed by Flügel (2010), during the phase of mechanical compaction before lithification, micrites with voids may be filled with calcite, forming a microfenestral fabric. It is therefore probable that during the diagenetic stages of several beds of the Del Monte Formation fluids were released contributing to both the development of the microfenestral fabric, as shown by the wackestone sample (Fig. 4A), and the development of the calcite or dolomite patches in the MF3 (Fig. 4H).

The occurrence of dolomitic limestone or dolostone microfacies (MF3) suggests that the original limestone was likely a wackestone (dolomitic), as evidenced by the occasional conspicuousness of a micritic matrix (Fig. 5h). Dolomitization probably occurred in FZ 8 (Wilson 1975), associated with the platform interior and corresponding to SMF 19 or 23 (Flügel 2010). This environment, probably enriched in Mg, facilitated dolomite transformation or replacement of calcareous components during the early diagenesis in a shallow basin deposition (e.g., Gyori et al. 2020). The presence of species of the genus *Diplognathodus* in bed CC54-11 which corresponds to MF3, indicates a quiet to moderately water-energy environment, likely in a restricted platform interior as Sweet (1988) reported. This suggests a facies change from a FZ in a high-energy platform margin to a quiet and restricted platform.

Although the mudstone microfacies (MF4) includes clay, silt, quartz content, and laminated structure composition, we can infer that it probably

originated in one of two environments according to Flügel's scheme. On one hand, it may have been deposited in a distal area of the deep shelf, possibly associated with the toe-of-slope, such as a pelagic mudstone (SMF 3; Flügel 2010). This assumption can probably be supported by the absence of bioclastic components, the micritic intraclasts, the olive-dark hues, and the opaque minerals of Fe-oxides of the stratigraphic level corresponding to sample CC54-04 (Fig. 5G), however, in contrast to pelagic mudstone microfacies, our sample preserves lamination. The laminations in mudstones are commonly developed from biogenetic or erosional processes that occur, for example, in moderately inclined basins with steeper slopes proximal FZ 3 (Wilson 1975; Fig. 6). On the other hand, micrites without fossils may also occur in a shallow marine environment, potentially in an intertidal zone with mudflats resembling those in FZ 8 (Wilson 1975) related to SMF 23 (Flügel 2010). Contrary to deeper laminated mudstones, the lamination of shallow mudstones are developed as a consequence of bedload transport during different episodes of sedimentation associated to tidal currents and in quiet conditions which contributes to the formation of these microfacies (e.g., Reineck & Singh 1980). However, further evidence is needed to determine the origin of this type of microfeatures.

Siliciclastic sandstone (MF5) is characterized by abundant poorly sorted detrital grains and a few benthic bioclasts, such as foraminifera and calcareous lithics (lc; Fig. 5A). These features indicate high energy with short transport, probably derived from the same platform and supplemented by detrital components from volcanic input (Casas-Peña et al. 2021). As in MF4, MF5 does not correspond to microfacies in the schemes of Wilson (1975) and Flügel (2010), which exclusively address pure carbonate rock. However, we can infer that the clastic inflow may have resulted from changes in sea level or deposition in sandbars and shoals formed under high-energy conditions in FZ 6 (Wilson 1975), near the fossiliferous platform margin (Fig. 6).

The field observations suggest that the calcareous breccia/conglomerate (calclithite *sensu* Folk 1959) Unit 2 of the Del Monte Formation (Fig. 2E) represents a proximal, high-energy deposit associated with a carbonate platform or possibly a submarine valley developed along a slope. This interpretation is supported by massive outcrops, occasional

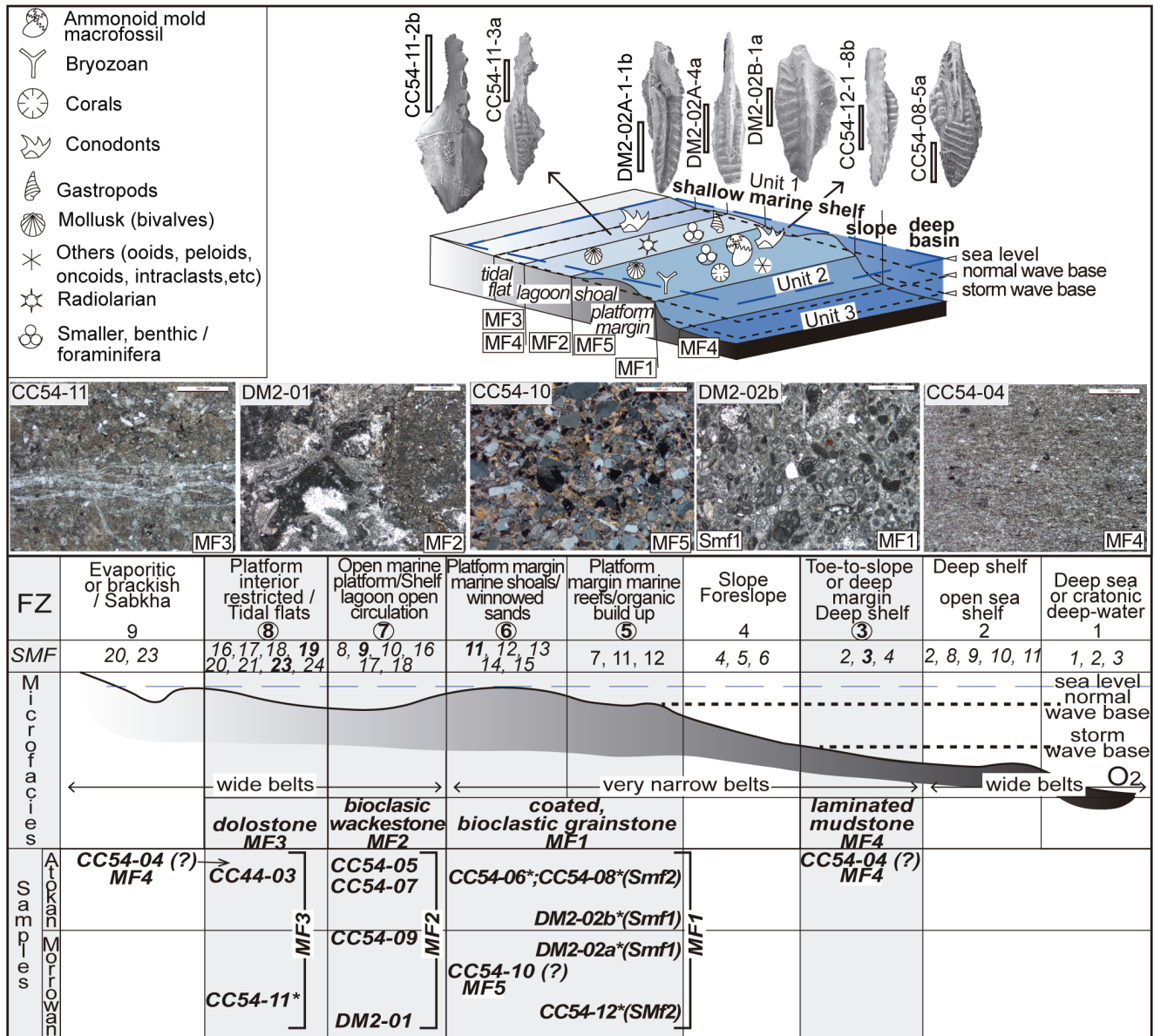


Fig. 6 - Schematic shallow marine platform model for the Pennsylvanian units of the Del Monte Formation of the Tamatán Basin showing the microfacies of the samples of Unit 1, the ages, and conodonts recognized.

graded grains, and carbonates and mud fragments resembling sedimentary constituents of Unit 1. Consequently, these characteristics imply that Unit 2 comprises submarine slope debris deposits (Fig. 6).

Unit 3 (Fig. 2F) of the Del Monte Formation is characterized by graded beds mostly appearing in intercalation with thin-bedded sandstone and shale beds with abundant quartz grain, suggesting that this turbiditic unit was originated in an open-marine basin environment related to deeper environments.

It should be noted that the basal unit considered as Naranjal Conglomerate by Carrillo-Bravo (1961) and Stewart et al. (1999a; Fig. 2G-H) lacks a clear stratigraphic relationship with surrounding

strata. While some authors (Ramírez-Ramírez 1992; Stewart et al. 1999a) consider it the basal unit of the Pennsylvanian Del Monte Formation and possibly with a olistostromal-related origin due to metamorphic and volcanic components, we propose an alternative view. The Naranjal Conglomerate shares similarities in framework, such as a reddish matrix and angular reddish sandy and volcanic fragments ranging from 0.5 cm to 20 cm, with Jurassic conglomerates found in the red beds of the La Joya Formation in southwestern Tamaulipas. These resemblances are also observed in the northernmost La Boca Canyon, both Caballeros and La Peregrina canyons of this study, and even further south in the

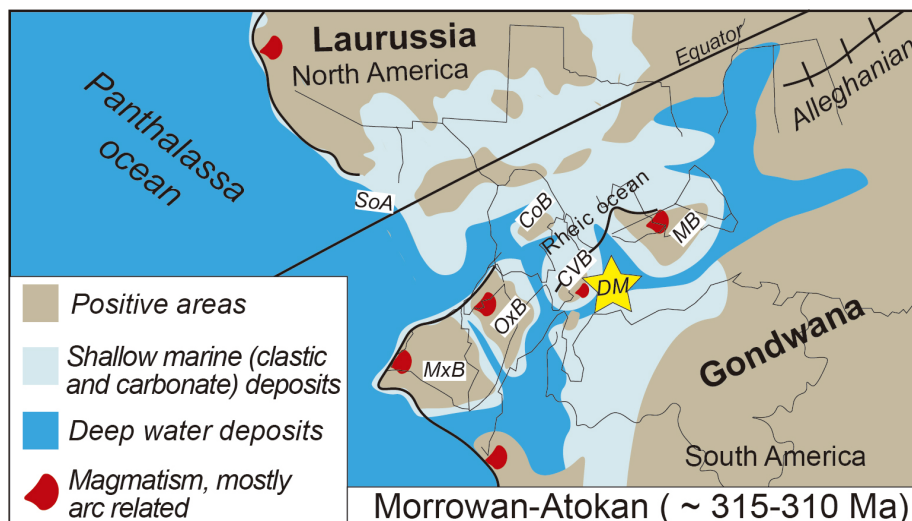


Fig. 7 - Paleogeographic conceptual model of the Del Monte Formation of Tamatán Basin and several Mexican peri-Gondwanan blocks during the Atokan – Morrowan (Modified from Miall and Blakey, 2019). Star: indicate the Del Monte Formation location (DM) Abbreviations. CoB: Coahuila Block, CVB: Ciudad Victoria Block, MB: Maya Block, MxB: Mixteco, OxB: Oaxaquia, SoA: Sonora Allochthon.

Valle del Huizachal, where the Huizachal Group has been defined (Barboza-Gudiño et al. 2011; Rubio-Cisneros et al. 2011). While this explanation is plausible, further studies are needed to precisely validate its accuracy.

Paleogeographic implications

The Carboniferous Period marked a crucial phase in Earth history, leading to the formation of the supercontinent Pangea. The movement of continental land masses and ongoing oceanic processes, including the closure of the Rheic and the Paleotethys oceans, had a profound impact on ocean circulation, climate, and tectonic evolution. These changes influenced various marine basins during the Carboniferous. The paleogeographic models of the Laurentia-Gondwana collision during the Carboniferous are widely accepted, supported by geophysical, sedimentological, and paleontological data from researchers like Hatcher (2002), Torsvik & Cocks (2004), Poole et al. (2005), Blakey (2008), and Miall & Blakey (2019). These models refer to the Laurentia-Gondwana collision tectonic event as a zipping-like closure which leads to the result of the Variscan, Alleghanian, and Marathon-Ouachita-Sonora orogenies. Furthermore, in the equatorial region, the Rheic Ocean remained as a corridor between the Paleotethys-Tethys and Panthalassa oceans, undergoing gradual closure from the Late Devonian to Early Permian. During the Carboniferous, the westernmost sector of the Rheic Ocean remained open. However, paleobiogeographic analyses on benthic foraminifera communities from North America and European Tethyan regions de-

monstrate that the formation of the Alleghanian isthmus took place during the Bashkirian (Early Pennsylvanian), closing the Rheic seaway (Davydov & Cozar 2019; Fig. 7).

PLATE 1

P1 elements of *Adetognathus*, *Diplognathodus*, *Idiognathoides*, and *Neognathodus* from Morrowan and Atokan ages of the Del Monte Formation in the Tamatán Group (Tamaulipas); scale bars are 200 μm . 1) *Adetognathus lantus* (Gunnell, 1933), Section 1 in the La Peregrina Canyon, sample specimen ERNO NP-DM2-02A-1-1b a 2) *Diplognathodus coloradoensis* (Murray & Chronic 1965), Section 1 in the La Peregrina Canyon, sample specimen ERNO NP-DM2-02A-2d; 3-5) *Idiognathoides convexus* (Ellison & Graves, 1941), section 2 in the Caballeros Canyon, sample specimens (3) ERNO NP-CC54-12-1-7a, (4) CC54-12-1-9a and Section 1 in the La Peregrina Canyon (5) ERNO NP-DM2-02A-1a; 6) *Idiognathoides corrugatus* Harris & Hollingsworth 1933, Section 3 in the Caballeros Canyon, sample specimen ERNO NP-CC54-06-6a; 7) *Idiognathoides* cf. *Id. corrugatus* Harris & Hollingsworth, 1933, Section 1 in the La Peregrina Canyon, sample specimen ERNO NP-DM2-02B-4a; 8-9) *Idiognathoides asiaticus* Nigmatganov & Nemyrovskaya, 1992, Section 2 in the Caballeros Canyon, sample specimens (8) ERNO NP-CC54-12-2b and (9) ERNO NP-CC54-11-3a; 10-14) *Idiognathoides sulcatus sulcatus* Higgins & Bouckaert, 1968, Section 1 in the La Peregrina Canyon, sample specimens (10) ERNO NP-DM2-02A-2d, (11) ERNO NP-DM2-02A-1-2a, (12) ERNO NP-DM2-02B-5a and from Section 2 in the Caballeros Canyon (13) ERNO NP-CC54-12-1-2b, (14) ERNO NP-CC54-12-1-8b; 15) *Neognathodus atokaensis* Grayson, 1984, Section 1 in the La Peregrina Canyon, sample specimen ERNO NP-DM2-02B-1a; 16) *Neognathodus atokaensis sensu* Lucas et al., 2017, Section 1 in the La Peregrina Canyon, sample specimen ERNO NP-DM2-02B-2a; 17-18) *Neognathodus* aff. *N. bothrops* Merrill, 1972, Section 2 in the Caballeros Canyon, sample specimens (17) ERNO NP-CC54-08-2a and (18) ERNO NP-CC54-08-7a; 19) *Neognathodus* cf. *N. expansus* (Jones, 1941), Section 2 in the Caballeros Canyon, sample specimen ERNO NP-CC54-08-1-2b.

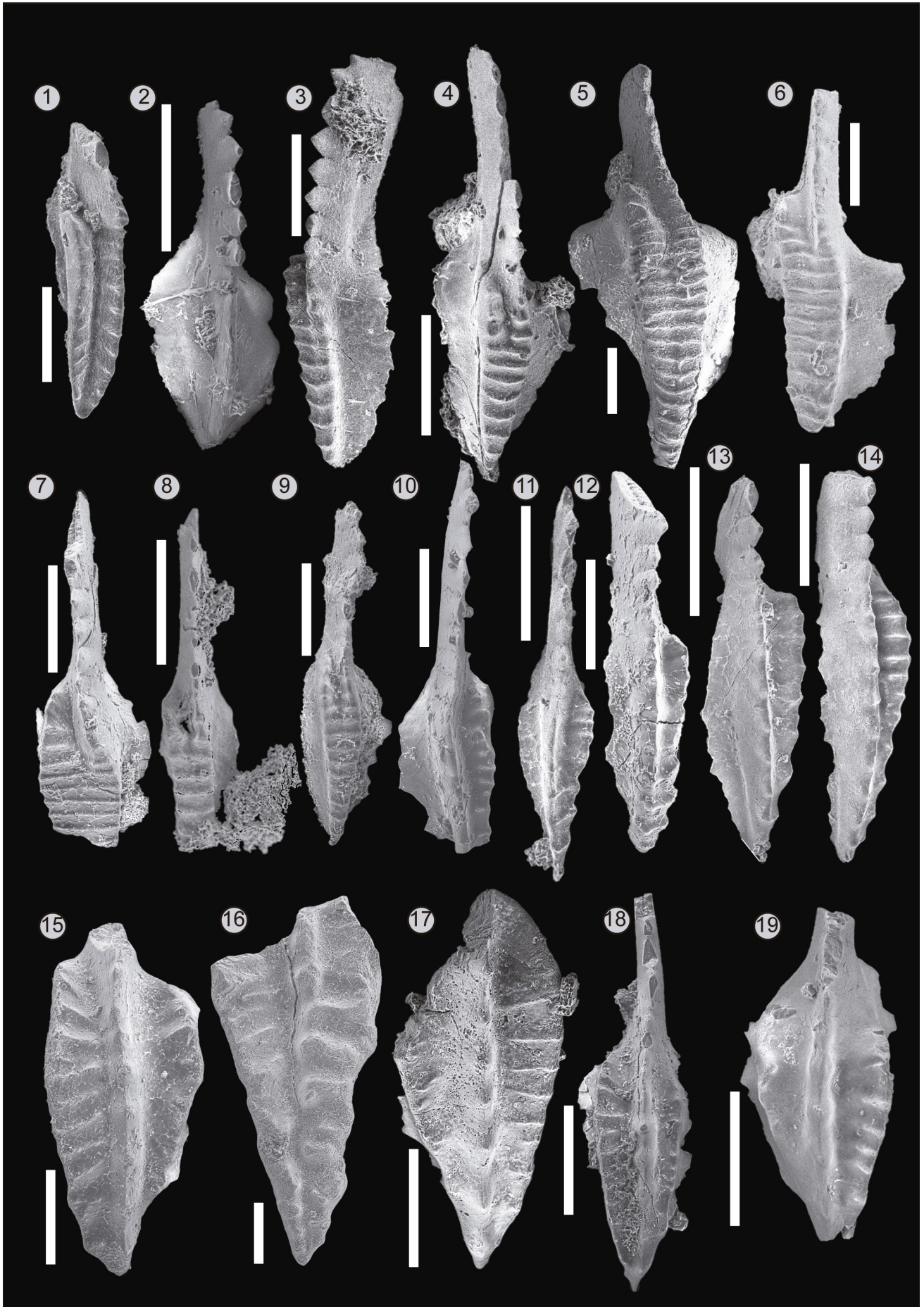


PLATE 1

These models, though, lack specific information about the Mexican terranes. The current territory of Mexico comprises several blocks, such as Oaxaquía, Mixteca, Maya, and the Ciudad Victoria Block, which are distributed on the periphery of northwestern Gondwana (Keppie et al. 2008). None of these models describes the depositional setting of the Tamatán Basin from the Ciudad Victoria Block or its relationship with neighboring basins.

Examining Pennsylvanian sedimentary successions in southeastern and northwestern Mexico, the Del Monte Formation exhibits similarities in lithology and fauna with these localities. In the Maya Block, the upper Santa Rosa Formation in Chiapas and the Santa Rosa Group in Guatemala show lithological similarities like turbidite deposits, even though identifiable fossils are absent (Clemons & Burkart 1971; Hernández-García 1973). The basins associated with the Oaxaquía Block, particularly the Ixtaltepec Formation in Oaxaca, contain carbonate terrigenous beds with diverse Carboniferous fauna, including bivalves, ammonoids, brachiopods and crinoids (Torres-Martínez & Sour-Tovar 2022). The Mixteca Block and the Pennsylvanian Patlanoaya Formation in Puebla show North American affinities in their lithology and fauna (e.g., crinoids, radiolarians) (Caridroit et al. 2002; Esquivel-Macías et al. 2004). Several specimens of *Streptognathodus bellus* Chernykh & Ritter, 1997 from a single sample were reported in this locality (Caridroit et al. 2002). In northwestern Mexico, the Carboniferous marine and siliciclastic succession represented by the Rancho Nuevo Formation, yield abundant fauna as well as conodonts which indicate deep-water strata of the Sonora Allochthon; besides fauna found in this formation is commonly related to that from the southern border of the United States or close to the cratonic platform of the southern part of Laurentia (Navas-Parejo 2018; Lara-Peña et al. 2020). In the central-eastern region of Sonora, the Sierra Agua Verde hosts a succession of Paleozoic rocks. These rocks were deposited in a carbonate platform environment and feature a diverse marine biota, including conodonts, phylloid algae, fusulinid foraminifera, chaetetid sponges, tabulate corals, gastropods, bryozoans, brachiopods, and crinoids (Stewart et al. 1999b). The Sierra Agua Verde Carboniferous succession includes the Mississippian/Pennsylvanian boundary (Navas-Parejo et al. 2017). Another noteworthy fossiliferous succession is found in the La

Horquilla Formation within the Pedregosa basin in Chihuahua, as documented by Wilson et al. (1969). Additionally, Carrillo-Bravo (1961) suggested a correlation with Pennsylvanian sediments in the southwest of Texas (Fig. 7).

Overall, the lithology and fossil records identified in the Pennsylvanian basins from northwestern Gondwana indicate a prevalence of marine facies primarily deposited in shallow marine environments. While the shallow marine facies dominate, there are instances of deep-marine deposits. Examples include the Santa Rosa Formation, the Rancho Nuevo Formation, and notably, the Del Monte Formation discussed in this study. These formations show the development or the initial deposition of turbiditic facies, suggesting a probable connection with deep-marine basins.

PLATE 2

Oral views of different P1 elements of *Neognathodus*, *Idiognathodus*, and *Streptognathodus* from Morrowan and Atokan ages of Del Monte Formation in the Tamatán Basin (Tamaulipas); scale bars are 200 μm . 1-2) *Neognathodus nataliae* Alekseev & Gerelzege, 2001 (in Alekseev and Goreva 2001), section 2 in the Caballeros Canyon sample specimens (1) ERNO NP-CC54-08-1-1a and Section 3 in the Caballeros Canyon, (2) ERNO NP-CC54-06-12b; 3-6 and 9-10) *Idiognathodus* aff. *I. delicatus* Gunnell, 1931, Section 2 in the Caballeros Canyon, sample specimens (3) ERNO NP-CC54-08-6a, (4) ERNO NP-CC54-08-4a, (5) ERNO NP-CC54-08-1b, (6) ERNO NP-CC54-08-14a, (9) ERNO NP-CC54-08-10a and from Section 3 in the Caballeros Canyon, sample specimen (10) ERNO NP-CC54-06-13a; 7-8 and 11, 17-18) *Idiognathodus incurvus* Dunn, 1966, Section 2 in the Caballeros Canyon, sample specimen (7) ERNO NP-CC54-08-5a and from Section 3, sample specimens (8) ERNO NP-CC54-06-10a, (11) ERNO NP-CC54-06-10b, (17) ERNO NP-CC54-06-5a and (18) ERNO NP-CC54-06-4a; 12-13) *Streptognathodus parvus* Dunn, 1966, Section 1 in the La Peregrina Canyon, sample specimens (12) ERNO NP-DM2-02A-4a and (13) ERNO NP-DM2-02B-3b; 14-15) *Idiognathodus* sp. A Grubbs, 1984, Section 2 in the Caballeros Canyon, sample specimens (14) ERNO NP-CC54-12-1b and (15) ERNO NP-CC54-12-3a; 16) *Idiognathodus* n. sp. B, Section 3 in the Caballeros Canyon, sample specimen ERNO NP-CC54-06-8a; 19) gerontic *Idiognathodus* n. sp. C, Section 3 in the Caballeros Canyon, sample specimen ERNO NP-CC54-06-15a; 20) gerontic *Idiognathodus* n. sp. C, Section 3 in the Caballeros Canyon, sample specimen ERNO NP-CC54-06-1b; 21) *Streptognathodus* n. sp., Section 2 in the Caballeros Canyon, sample specimen ERNO NP-CC54-08-9a; 22-23) Ichthyoliths, sample specimens (22) ERNO NP-CC54-12-4a and (23) ERNO NP-DM2-02B-6a.

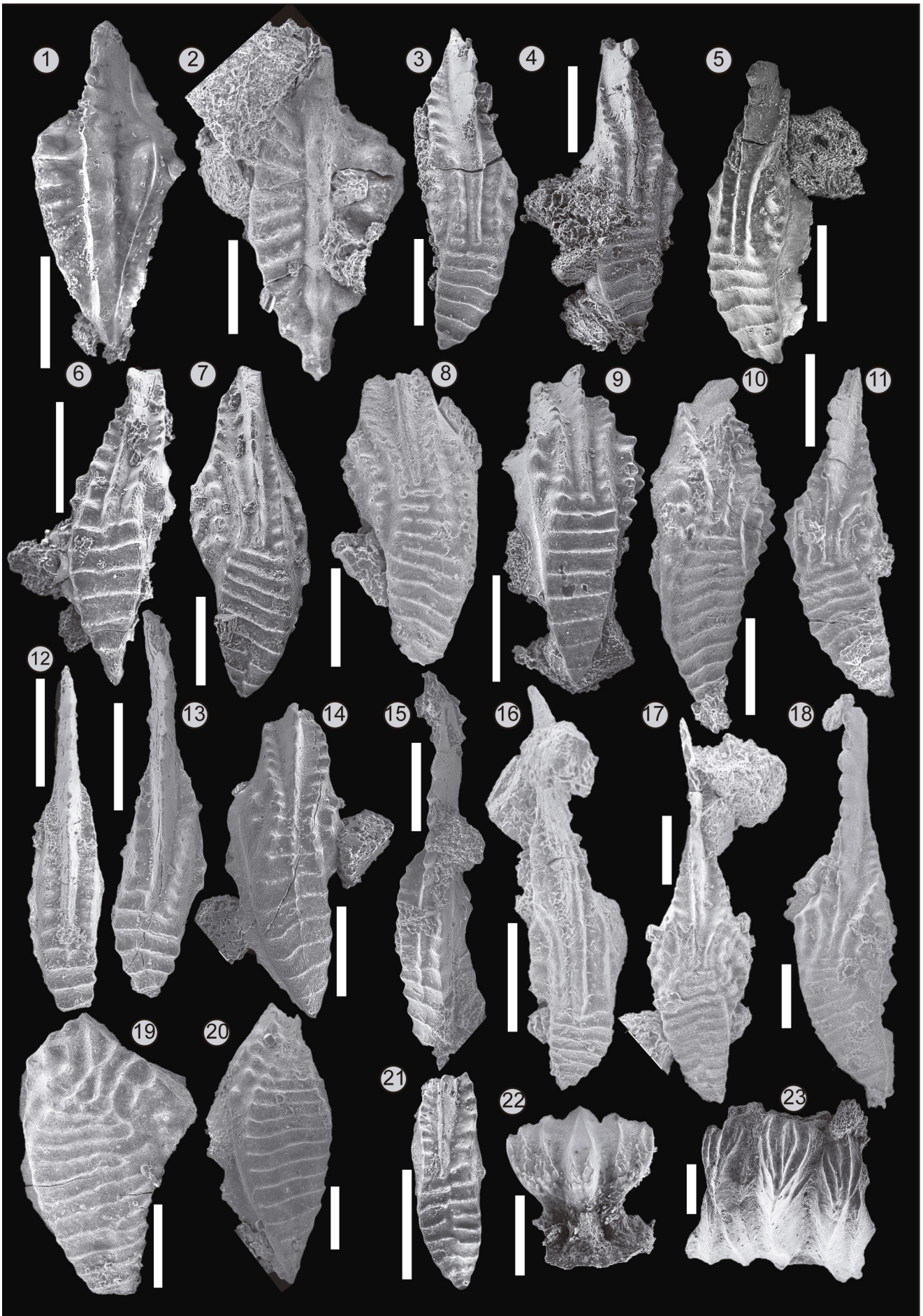


PLATE 2

The Pennsylvanian sediments from the Tamatán Basin, associated with the Ciudad Victoria Block and represented by the Del Monte Formation, plausibly followed a global trend with alternations of limestone, shale, and sandstone. The development of shallow conditions related to platforms and ramps and then transitioned to slopes and deeper basins with turbidites development, perhaps was influenced by the transgressive and regressive phases under glacial eustatic control (Heckel 1990) in the Middle Pennsylvanian. These sea-level changes resulted in the development of two environments associated with the shallow marine platform, one with a restricted environment (e.g. sample CC54-11) and another of outer edge of the platform near the slope (e.g. CC54-12 and DM2-02A samples), indicating relatively rapid marine fluctuation in the Morrowan, and which also maintained this trend in the Atokan (Fig. 6). Additionally, the Del Monte Formation, like other Mexican peri-Gondwanan basins shows an abundant input of volcanic material derived from several magmatic sources that occurred during the Carboniferous (Fig. 7).

CONCLUSIONS

The geological insights obtained from conodont biostratigraphic analysis, microfacies, and field observations within the Del Monte Formation offer valuable information on its age and depositional environments, and paleogeographic implications that can be summarized as follows.

The Del Monte Formation includes three distinct units: Unit 1, containing alternating carbonatic and siliciclastic deposits; Unit 2, characterized by basal conglomerate/breccia as calcareous debris deposits; and Unit 3, consisting of turbiditic sandstone and shale.

Conodonts species such as *Adetognathus lautus*, *Idiognathoides corrugatus*, *Id. sulcatus sulcatus*, *Id. convexus*, *Id. asiaticus*, *Diplognathodus coloradoensis*, *Neognathodus atokaensis*, *N. aff. bothrops*, *N. nataliae*, *Idiognathodus incurvus*, and *Streptognathodus parvus* within bioclastic grainstone and dolostone levels of Unit 1 indicate Morrowan and Atokan ages.

Five microfacies in Unit 1 consist of predominantly bioclastic grainstone with few occurrence of wackestone and dolostone. This suggests depositional environments associated with both the platform margin and a more restricted interior platform.

The geological model of a carbonate platform associated to a slope and an open marine environment for the Del Monte Formation is supported by the presence of debris flow-slope and turbidite deposits in Unit 2 and Unit 3.

The preservation of shallow and deep marine basins in other Mexican peri-Gondwanan basins in the Pennsylvanian, provides evidence for seaways prior to the complete closure of the Rheic Ocean, with a possible connection with the Tamatán Basin.

Acknowledgements: The first author (J.M.C.-P.) acknowledges the postdoctoral program of the Dirección General de Asuntos del Personal Académico, Universidad Nacional Autónoma de México (DGAPA-UNAM) and the Estación Regional del Noroeste, Instituto de Geología (ERNO-IGL, UNAM). We acknowledge suggestions and comments of Francisco Sour Tovar and of an anonymous reviewer, that significantly enriched the original manuscript. We also thank Francesca Bosellini and Lucia Angiolini whose comments and editorial work greatly improved our work. In the same way, we are deeply grateful to Robert Blodgett for his review. Special thanks to V.A. Leal-Cuellar (FCT, UANL) and E.A. Alemán-Gallardo (ICBI, UAEH) for their support during fieldwork. We also thank Aimée Orci Romero (ERNO-IGL, UNAM) for the preparation of thin sections. We are thankful to Laboratorio Nacional de Geoquímica y Mineralogía (LANGEM) at ERNO and Daniel Ramos Perez for his technical support for SEM image acquisition. Financial support for this work was provided by PAPIIT DGAPA-UNAM (project IN114923 granted to P. N-P). This work is also a contribution to CONAHCYT Ciencia de Frontera project 7351.

REFERENCES

- Alekseev A.S. & Goreva N.V. (2001) - Chapter 9 – Conodonts. In: Makhlina M.K. et al. (Eds) Middle Carboniferous of Moscow Syncline (southern part). Volume 2. Biostratigraphy:113–140. Scientific World, Moscow. [In Russian]
- Alemán-Gallardo E., Ramírez Fernández J.A., Rodríguez Díaz, A. Velasco-Tapia F., Jenchen U., Cruz-Gómez E., Navarro-de León I. & de Leon-Barragán L. (2019a) - Evidence for an Ordovician continental arc in the pre-Mesozoic basement of the Huizachal-Peregrina Anticlinorium, Sierra Madre Oriental, Mexico: the Peregrina Tonalite. *Mineralogy and Petrology*, 113 (4): 433–562.
- Alemán-Gallardo E.A., Ramírez-Fernández J.A., Weber B., Velasco-Tapia F. & Casas-Peña J.M. (2019b) - Novillo Metamorphic Complex, Huizachal-Peregrina Anticlinorium, Tamaulipas, Mexico: Characterization and development based on whole-rock geochemistry and Nd-isotopic ratios. *Journal of South American Earth Sciences*, 96 (102382): 1–17.
- Barboza-Gudiño J.R., Ramírez-Fernández J.A., Torres-Sánchez S.A. & Valencia V.A. (2011) - Geocronología de circones detríticos de diferentes localidades del Esquisto Granjeno en el noreste de México. *Boletín de la Sociedad Geológica Mexicana*, 63 (2): 201–216.
- Barrick J.E., Alekseev A.S., Blanco-Ferrera S., Goreva N.V., Hu K., Lambert L.L., Nemyrovska T.I., Qi Y., Ritter

- S.M. & Sanz-López J. (2022) - Carboniferous conodont biostratigraphy. *Geological Society, London, Special Publications*, 512: 695–768.
- Barrick J.E., Lambert L.L., Heckel P.H., Rosscoe S.J. & Boardman D.R. (2013) - Midcontinent Pennsylvanian conodont zonation. *Stratigraphy*, 10: 55–72.
- Blakey R.C. (2008) - Gondwana paleogeography from assembly to break up – 500 m.y. odyssey. In: Fielding C.R., Frank, T.D. & Isbell J.L. (Eds) - *Resolving the Late Paleozoic Ice Age in Time and Space*, Geological Society of America Special Paper, 441: 1–28.
- Boucot A.J., Benedetto J.L., Grahn Y., Melo J.H.G., Sanchez T.M. & Waisfeld B.A. (1999) - South American marine Silurian communities. In: Boucot A.J. & Lawson J.D. (Eds) - *Final Report, Project Ecostratigraphy. Paleocommunities – a case study from the Silurian and Lower Devonian*: 841–848. Cambridge University Press, Cambridge.
- Boucot A.J., Blodgett R.B., & Stewart J.H. (1997) - European Province Late Silurian brachiopods from the Ciudad Victoria area, Tamaulipas, northeastern Mexico. In: Klapper G., Murphy M.A. & Talent J.A. (Eds) - *Paleozoic sequence stratigraphy, biostratigraphy, and biogeography: Studies in honor of J. Granville (“Jess”) Johnson*, *Geological Society of America Special Paper* 321: 273–293.
- Brown L.M., Rexroad C.B. & Zimmerman A.N. (2016) - Conodont paleontology of the Alum Cave Limestone Member of the Dugger Formation (Pennsylvanian, Desmoinesian) in the eastern part of the Illinois Basin. *Indiana Geological Survey Occasional Paper*, 72: 25 pp.
- Campa M.F. & Coney P.J. (1982) - Tectonostratigraphic terranes and mineral resource distributions in Mexico. *Canadian Journal of Earth Sciences*, 20: 1040–1051.
- Cardoso C.N., Sanz-López J. & Blanco-Ferrera S. (2017a) - Pennsylvanian conodonts from the Tapajós Group, Amazonas Basin (Brazil). *Geobios*, 50: 75–95.
- Cardoso C.N., Sanz-López J. & Blanco-Ferrera S. (2017b) - Pennsylvanian conodont zonation of the Tapajós Group (Amazonas Basin, Brazil). *Stratigraphy*, 14: 35–58.
- Caridroit M., Lamerand A., Dégardin J.M., Flores de Dios A. & Vachard D. (2002) - Discovery of radiolaria and conodonts in the Carboniferous–Permian of San Salvador Patlanoaya (Puebla, Mexico); biostratigraphic implications. *Comptes Rendus Palevol*, 1: 205–211.
- Carrillo-Bravo J. (1961) - Geología del Anticlinorio Huizachal-Peregrina al NW de Ciudad Victoria, Tamps. *Boletín de la Asociación Mexicana de Geólogos Petroleros*, 13 (1/2): 1–98.
- Casas-Peña J.M., Ramírez-Fernández J.A., Velasco-Tapia F., Alemán-Gallardo E.A., Augustsson C., Weber B., Frei D. & Jenchen U. (2021) - Provenance and tectonic setting of the Paleozoic Tamatán Group, NE Mexico: Implications for the closure of the Rheic Ocean. *Gondwana Research*, 91: 205–230.
- Chernykh V.A. & Ritter S.M. (1997) - *Streptognathodus* (Conodonts) succession at the proposed Carboniferous–Permian Boundary Stratotype Section, Aidaralash Creek, northern Kazakhstan. *Journal of Paleontology*, 71(3): 459–474.
- Clemons R.E. & Burkart B. (1971) - Stratigraphy of northwestern Guatemala. *Boletín de la Sociedad Geológica Mexicana*, 32 (2): 143–158.
- Davydov V.I. & Cózar P. (2019) - The formation of the Alleghenian Isthmus triggered the Bashkirian glaciation: Constraints from warm-water benthic foraminifera. *Palaogeography, Palaeoclimatology, Palaeoecology*, 531: 108403.
- Davis L.E. & Webster G.D. (1985) - Late Mississippian to Early Pennsylvanian conodont biofacies in central Montana. *Letabaia*, 18: 67–72.
- Dunham R.J. (1962) - Classification of carbonate rocks according to their depositional texture. In: Ham W.E. (Eds) - *Classification of Carbonate Rocks*: 108–121. American Association of Petroleum Geologists, Tulsa.
- Dunn D.L. (1966) - New Pennsylvanian platform conodonts from southwestern United States. *Journal of Paleontology*, 40: 1294–1303.
- Dunn D.L. (1970a) - Conodont zonation near the Mississippian–Pennsylvanian boundary in Western United States. *Geological Society of America Bulletin*, 81: 2959–2974.
- Dunn D.L. (1970b) - Middle Carboniferous conodonts from western United States and phylogeny of the platform group. *Journal of Paleontology*, 44: 312–342.
- Ellison S.P. (1941) - Revision of the Pennsylvanian conodonts. *Journal of Paleontology*, 15: 107–143.
- Ellison S.P. & Graves R.W.Jr (1941) - Lower Pennsylvanian (Dimple Limestone) conodonts of the Marathon region, Texas. *Metallurgy Bulletin Technical Series*, University of Missouri School of Mines and Metallurgy, 14 (3): 13 pp.
- Embry A.F. & Klovan J.E. (1971) - A Late Devonian reef tract on northeastern Banks Island, N.W.T. 1. *Bulletin of Canadian Petroleum Geology*, 19: 730–781.
- Esquivel-Macías C., Solís-Marín F. & Buitrón-Sánchez B.E. (2004) - Nuevos registros de placas columnares de crinoideos (Echinodermata, Crinoidea) del Paleozoico Superior de México, algunas implicaciones paleobiogeográficas y paleoambientales. *Coloquios de Paleontología*, 54: 15–23.
- Flügel E. (2010) - *Microfacies of carbonate rocks, analysis, interpretation, and application*. Springer-Verlag, Berlin, 976 pp.
- Fohrer B, Nemyrovska T.I., Samankassou E., & Ueno K. (2007) - The Pennsylvanian (Moscovian) Izvarino Section, Donets Basin, Ukraine: A multidisciplinary study on microfacies, biostratigraphy (conodonts, foraminifers, and ostracodes), and paleoecology. *Journal of Paleontology*, 81 (sp69): 1–85.
- Folk R.L. (1959) - Practical petrographic classification of limestones. *Bulletin of American Association of Petroleum Geologists*, 43 (1): 1–38.
- Folk R.L. (1962) - Spectral subdivision of limestone types. In: Ham W.E. (Eds) - *Classification of Carbonates Rocks - A Symposium*: 62–84. American Association of Petroleum Geologists Memoir.
- Gomez-Rivas E., Martín-Martín J.D., Bons P.D., Koehn D., Griera A., Trav A., Llorens M.G., Humphrey E. & Neilson J. (2022) - Stylolites and stylolite networks as primary controls on the geometry and distribution of carbonate diagenetic alterations. *Marine and Petroleum Geology*, 136 (2022): 105444.
- Grayson R.C., Jr. (1984) - Morrowan and Atokan (Pennsylvanian) conodonts from the northeastern margin of the Arbuckle Mountains, Southern Oklahoma. In: Sutherland P.K. & Manger W.L. (Eds) - *The Atokan Series (Pennsylvanian) and its boundaries-A symposium*, 136: 41–63. Oklahoma Geological Survey Bulletin.
- Grubbs R.K. (1984) - Conodont platform elements from the Wapanucka and Atoka Formations (Morrowan-Atokan)

- of the Mill Creek Syncline, central Arijuckle Mountains, Oklahoma. In: Sutherland P.K. & Manger W.L. (Eds) - The Atokan Series (Pennsylvanian) and its boundaries: a Symposium, Geological Survey Oklahoma Bulletin 136: 65–79.
- Gunnell F.H. (1931) - Conodonts from the Fort Scott Limestone of Missouri. *Journal of Paleontology*, 5 (3): 244–252.
- Gunnell F.H. (1933) Conodonts and Fish Remains from the Cherokee, Kansas, City, and Wabaunsee Groups of Missouri and Kansas. *Journal of Paleontology*, 7 (3): 261–297.
- Gursky H.J. (1996) - Paleozoic stratigraphy of the La Peregrina canyon area, Sierra Madre Oriental, NE Mexico. *Zentralblatt für Geologie und Paläontologie, Teil I: Allgemeine, Angewandte, Regionale und Historische Geologie*, (7–8): 973–989.
- Gursky H.J. & Michalzik D. (1989) - Lower Permian turbidites in the northern Sierra Madre Oriental, Mexico. *Zentralblatt für Geologie und Paläontologie, Teil I: Allgemeine, Angewandte, Regionale und Historische Geologie*, (5–6): 821–838.
- Gyori O., Haas J., Hips K., Lukoczki G., Budai T., Demény A. & Szocs E. (2020) - Dolomitization of shallow-water, mixed siliciclastic-carbonate sequences: The Lower Triassic ramp succession of the Transdanubian Range, Hungary. *Sedimentary Geology*, 295: 105549.
- Harris R.W. & Hollingsworth R.V. (1933) - New Pennsylvanian conodonts from Oklahoma. *American Journal of Science*, 225: 193–204.
- Hatcher R.D. (2002) - Alleghanian (Appalachian) orogeny, a product of zipper tectonics: Rotational transpressive continent-continent collision and closing of ancient oceans along irregular margins. In: Martínez-Catalán J.R., Hatcher R.D., Arenas R. & Díaz-García F. (Eds) - Variscan-Appalachian Dynamics: The building of the late Paleozoic basement, Geological Society of America, Special Paper, 364: 199–208.
- Heckel P.H. (1990) - Evidence for global (glacial-eustatic) control over upper Carboniferous (Pennsylvanian) cyclothems in midcontinent North America. In: Hardman R.F.P. & Brooks J. (Eds) - Tectonic Events Responsible for Britain's 35 Oil and Gas Reserves. *Geological Society Special Publication*, 55: 35–47.
- Heckel P.H. (1994) - Evaluation of evidence for glacial-eustatic control over marine Pennsylvanian cyclothems in North America and consideration of possible tectonic effects. *SEPM Concepts in Sedimentology and Paleontology*, 4: 65–87.
- Hernández-García R. (1973) - Paleogeografía del Paleozoico de Chiapas, México. *Boletín de la Asociación Mexicana de Geólogos Petroleros*, 25: 79–113.
- Higgins A.C. & Bouckaert J. (1968) - Conodont stratigraphy and palaeontology of the Namurian of Belgium. *Mémoires pour Servir à l'Explication des Cartes Géologiques et Minières de la Belgique*, (10): 1–64.
- Hu K.Y., Qi Y.P., Wang Q.L., Nemyrovska T.I. & Chen J.T. (2016) - Early Pennsylvanian conodonts from the Luokun section of Luodian, Guizhou, South China. *Palaeworld*, 26: 64–82.
- Jones D.L. (1941) - The conodont fauna of the Seminole Formation. *University of Chicago Libraries, Chicago, Illinois*, 55 pp.
- Keppie J.D., Dostal J., Miller B.V., Ramos-Arias M.A., Morales-Gámez M., Nance R.D., Murphy J.B., Ortega-Rivera A., Lee J.W.K., Housh T. & Cooper P. (2008) - Ordovician–earliest Silurian rift tholeiites in the Acatlán Complex, southern Mexico: Evidence of rifting on the southern margin of the Rheic Ocean. *Tectonophysics*, 461: 130–156.
- Lane H. R., Merrill G. K., Straka J.J. II. & Webster D. (1970) - North American Pennsylvanian Conodont Biostratigraphy. In: Stweet W.C. & Bergstrom S.M (Eds) - *Symposium on Conodont Biostratigraphy*. Geological Society America memoirs, 127: 395–412.
- Lane H.R. & Straka, J.J. II (1974) - Late Mississippian and Early Pennsylvanian conodonts, Arkansas and Oklahoma. In: Lane H.R. & Straka J.J. II (Eds) - Late Mississippian and Early Pennsylvanian conodonts, Arkansas and Oklahoma. Geological Society America Special Paper, 152: 1–144.
- Lara-Peña R.A. Navas-Parejo P. & Amaya-Martínez R. (2020) - New conodont data related to the western Ouachita-Marathon-Sonora orogen: Age of the autochthonous Laurentian deformation. *Journal of South American Earth Sciences*, 103: 102763.
- Léveillé C. (1835) - Aperçu géologique de quelques localités très riches en coquilles sur les frontières de la France de Belgique. *Mémoires de la Société Géologique de la France*, 2: 29–40.
- Lucas S.G., Dimichele W.A. Krainer K., Barrick J.E., Vachard D., Donovan M.P., Looy C., Kerp H. & Chaney D.S. (2021) - The Pennsylvanian System in the northern Sacramento Mountains, New Mexico, USA: stratigraphy, petrography, depositional systems, paleontology, biostratigraphy and geologic history. *Smithsonian Contributions to Paleobiology*, 104.
- Lucas S.G., Krainer K., Barrick J.E., Vachard D. & Ritter S.M. (2017) - Lithostratigraphy and microfossil biostratigraphy of the Pennsylvanian–lower Permian Horquilla Formation at New Well Peak, Big Hatchet Mountains, New Mexico, USA. *Stratigraphy*, 14: 223–246.
- Malpica C.R. & De La Torre L.G (1980). Integración estratigráfica del Paleozoico de México, Proyecto C-1079, Parte I - México. *Instituto Mexicano del Petróleo*: pp. 267.
- Merrill G.K. (1972) - Taxonomy, Phylogeny, and Biostratigraphy of *Neognathodus* in Appalachian Pennsylvanian Rocks. *Journal of Paleontology*, 46 (6): 817–829.
- Miall A.D. & Blakey R.C. (2019) - Chapter 1 – The Phanerozoic Tectonic and Sedimentary Evolution of North America. *The Sedimentary Basins of the United States and Canada*, 2: 1–38.
- Murray F.N. & Chronic J. (1965) - Pennsylvanian conodonts and other fossils from the insoluble residues of the Minturn Formation (Desmoinesian), Colorado. *Journal of Paleontology*, 39: 594–610.
- Murray G.E., Furnish W.M. & Carrillo B.J. (1960) - Carboniferous goniatites from Caballeros Canyon, State of Tamaulipas, Mexico. *Journal of Paleontology*, 34 (4): 731–737.
- Navas-Parejo P. (2018) - Carboniferous biostratigraphy of Sonora: a review. *Revista Mexicana de Ciencias Geológicas*, 35 (1): 41–53.
- Navas-Parejo P., Palafox-Reyes J.J., Villanueva R., Buitrón-Sánchez B.E. & Valencia-Moreno M. (2017) - Mid-Carboniferous conodonts from northwest Mexico. *Micropaleontology*, 63: 383–402.
- Nemyrovska T.I. (1999) - Bashkirian conodonts of the Donets Basin, Ukraine. *Scripta Geologica*, 119: 1–115.
- Nemyrovska T.I., Wagner R.H., Winkler Prins C.F. &

- Montañez I. (2011) - Conodont faunas across the mid-Carboniferous boundary from the Barcaliente Formation at La Lastra (Palentian Zone, Cantabrian Mountains, northwest Spain); geological setting, sedimentological characters, and faunal descriptions. *Scripta Geologica*, 143: 127–183.
- Nigmatganov I.M. & Nemyrovskaya T.I. (1992) - Mid-Carboniferous Boundary Conodonts from the Gissar Ridges, South Tianshan, Middle Asia. *Courier Forschungsinstitut Senckenberg*, 154: 253–275.
- Ortega-Gutiérrez F., Elías-Herrera M., Morán-Zenteno D.J., Solari L., Weber B. & Luna-González L. (2018) - The pre-Mesozoic metamorphic basement of Mexico, 1.5 billion years of crustal evolution. *Earth-Science Reviews*, 183: 2–37.
- Poole F.G., Perry Jr., W.J., Madrid R.J. & Amaya-Martínez R. (2005) - Tectonic synthesis of the Ouachita-Marathon-Sonora orogenic margin of southern Laurentia: stratigraphic and structural implications for timing of deformational events and plate-tectonic model. In: Anderson T.H., Nourse J.A., Mckee J.W. & Steiner M.B. (Eds) - The Mojave-Sonora Megashield Hypothesis: Development, Assessment, and Alternatives, Geological Society of America Special Paper, 393: 543–596.
- Qi Y.P., Lambert L.L., Nemyrovskaya T.I., Wang X.D., Hu K.Y. & Wang Q.L. (2015) - Late Bashkirian and early Moscovian conodonts from the Naqing section, Luodian, Guizhou, South China. *Palaeoworld*, 25: 170–187.
- Ramírez-Fernández J.A., Alemán-Gallardo E.A., Cruz-Castillo D., Velasco-Tapia F., Jenchen U., Becchio R., De León-Barragán L., & Casas-Peña J.M. (2021) - Early Mississippian pre-collisional, peri-Gondwanan volcanic arc in NE-Mexico: Aseradero Rhyolite from Ciudad Victoria, Tamaulipas. *International Journal of Earth Sciences*, 110: 2435–2463.
- Ramírez-Ramírez C. (1992) - Pre-Mesozoic geology of Huizachal-Peregrina Anticlinorium, Ciudad Victoria, Tamaulipas, and adjacent parts of eastern Mexico. PhD thesis, Texas University, Austin, Texas.
- Reineck H.E. & Singh I.B. (1980) - Depositional Environments. In: Reineck H.E. & Singh I.B. (Eds) - Depositional Sedimentary Environments: With reference to Terrigenous Clastics, 546: 4–6. Springer-Verlag, Berlin, Heidelberg, New York.
- Roscoe S.J. (2005) - Conodonts of the Desmoinesian (Middle Pennsylvanian) Lost Branch Formation, Oklahoma and Kansas. Master Thesis. Texas Tech University.
- Roscoe S.J. & Barrick J.E. (2009) - Revision of *Idiognathodus* species from the Desmoinesian–Missourian (~Moscovian–Kasimovian) boundary interval in the Midcontinent Basin, North America. In: Over D.J. (Eds) - Conodont studies commemorating the 150th anniversary of the first conodont paper (Pander 1856) and the 40th anniversary of the *Pander Society*. *Palaeontographica Americana*, 62: 115–147.
- Rowley R.R. (1900) - Descriptions of new species of fossils from Devonian and Sub-Carboniferous rocks of Missouri. *The American Geologist*, 25 (5): 261–273.
- Rubio-Cisneros I.I., Ramírez-Fernández J.A. & García-Obregón R. (2011) - Análisis preliminar de procedencia de rocas clásticas jurásicas del valle de Huizachal, Sierra Madre Oriental: Influencia del vulcanismo sinsedimentario y el basamento cristalino. *Boletín de la Sociedad Geológica Mexicana*, 63 (2): 137–156.
- Sedlock R.L., Ortega-Gutiérrez F. & Speed R.C. (1993) - Tectonostratigraphic terranes and tectonic evolution of Mexico. *Geological Society of America Special Paper*, 278: 142 pp.
- Skinner J.W. & Wilde G.L. (1954) - New early Pennsylvanian Fusulinids from Texas. *Journal of Paleontology*, 28(6): 796–803.
- Sour-Tovar F. & Martínez-Chacón M.L. (2004) - Braquiópodos chonetoideos del Carbonífero de México. [Chonetoidea (Brachiopoda) from the Carboniferous of Mexico]. *Revista Española de Paleontología*, 19 (2): 125–138.
- Sour-Tovar F., Álvarez F. & Martínez Chacón M.L. (2005) - Lower Mississippian (Osagean) spire-bearing brachiopods from Cañón de la Peregrina, North of Ciudad Victoria, Tamaulipas, northeastern México. *Journal of Paleontology*, 79 (3): 469–485.
- Stauffer C.R. & Plummer H.J. (1932) - Texas Pennsylvanian conodonts and their stratigraphic relations. *The University of Texas Bulletin*, 3201: 13–50.
- Stewart J.H., Blodgett R.B., Boucot A.J., Carter J.L. & Lopez R. (1999a) - Exotic Paleozoic strata of Gondwanan provenance near Ciudad Victoria, Tamaulipas, Mexico. In: Ramos V.A. & Keppie J.D. (Eds) - Laurentia-Gondwana connections before Pangea, *Geological Society of America Special Paper*, 336: 227–252.
- Stewart J.H., Poole F.G., Harris A.G., Repetski J.E., Wardlaw B.R., Mamet B. & Morales-Ramírez J.M. (1999b) - Neoproterozoic(?) to Pennsylvanian inner-shelf, miogeoclinal strata in Sierra Agua Verde, Sonora, Mexico. *Revista Mexicana de Ciencias Geológicas*, 16: 35–62.
- Stone J. (1987) - Review of investigative techniques used in the study of conodonts. In: Austin R.L. (Ed) - Conodonts: Investigative techniques and applications: 17–34. Chichester, Ellis Horwood Limited.
- Sungatullina G. (2014) - Determination of the Bashkirian–Moscovian boundary in the Volga region via conodont species *Declinognathodus donetzianus* Nemyrovskaya. *Geological Magazine*, 151 (2): 299–310.
- Swade J.W. & Heckel P.H. (1985) - Conodont distribution, paleoecology, and preliminary biostratigraphy of the Upper Cherokee and Marmaton Groups (upper Desmoinesian, Middle Pennsylvanian) from Two Cores in South-Central Iowa. *Iowa Geological Survey, Technical Information Series*, 14: 1–71.
- Sweet W.C. (1988) - The Conodonta: Morphology, Taxonomy, Paleoecology and Evolutionary History of a Long-Extinct Animal Phylum – Oxford Monographs on Geology and Geophysics, Oxford University Press, London, 10: 205pp.
- Thomas H.D. (1928) - An Upper Carboniferous fauna from the Amotape Mountains, north-western Peru. *Geology Magazine*, 65: 146–152.
- Thompson T.L. & Lambert L.L. (2017) - Atokan (Middle Pennsylvanian) conodonts from laterally restricted pre-Cherokee units of southwestern Missouri. *Stratigraphy*, 14: 377–389.
- Torres-Martínez M.A., & Sour-Tovar F. (2022) - New rhynchonellid and spire-bearing brachiopods from the Carboniferous of Mexico. Paleogeographical significance of the Oaxacan brachiopod fauna through the Serpukhovian–Moscovian. *Journal of Paleontology*, 97 (1): 1–22.
- Torres-Sánchez S.A., Augustsson C., Jenchen U., Barboza-Gudiño J.R., Alemán-Gallardo E., Ramírez-Fernández

- J.A., Torres-Sánchez D. & Abratis M. (2017) - Petrology and geochemistry of meta-ultramafic rocks in the Paleozoic Granjeno Schist, northeastern Mexico: Remnants of Pangaea ocean floor. *Open Geoscience*, 9: 361–384.
- Torsvik T.H. & Cocks L.R.M. (2004) - Earth geography from 400 to 250 Ma: a paleomagnetic, faunal and facies review. *Journal of the Geological Society*, 161: 555–572.
- Vandeginste V. & John C.M. (2013) - Diagenetic implications of stylolitization in pelagic carbonates, Canterbury Basin, offshore New Zealand. *Journal of Sedimentary Research*, 83 (3): 226–240.
- Wilson J.L., Madrid-Solis A. & Malpica-Cruz R. (1969) - Microfacies of Pennsylvanian and Wolfcampian strata in southwestern U.S.A. and Chihuahua, Mexico. In: Cordoba D.A., Wengerd S.A. & Shomaker J.W. (Eds) - New Mexico Geological Society 20th Annual Fall Field Conference Guidebook, 80–90: 228pp. New Mexico Geological.
- Wilson N.J.L. (1975) - Carbonate Facies in Geologic History. Berlin: Springer-Verlag: 411 pp.